

AD 633841

HEL 2-12



# A FUNCTION FOR SAND MOVEMENT BY WIND

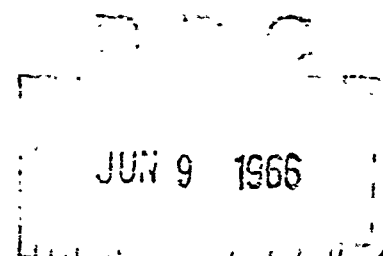
by

A. A. KADIB

CLEARINGHOUSE FOR FEDERAL SCIENTIFIC AND TECHNICAL INFORMATION			
Hardcopy	Microfiche		
\$ 4.00	\$ .75	103	3002
ARCHIVE COPY			

PROCESSING COPY

Code 1



Am



HYDRAULIC ENGINEERING LABORATORY  
WAVE RESEARCH PROJECTS

UNIVERSITY OF CALIFORNIA  
BERKELEY, CALIFORNIA  
JANUARY, 1965

University of California  
Hydraulic Engineering Laboratory

Submitted under Contract DA-49-055-CIV-ENG-63-4 with the  
Coastal Engineering Research Center, U.S. Army

Institute of Engineering Research  
Technical Report  
HEL-2-12

A FUNCTION FOR SAND MOVEMENT BY WIND

by

A.A. Kadib

Berkeley, California  
January 1965

## TABLE OF CONTENTS

	<u>Page</u>
Abstract . . . . .	i
List of Figures . . . . .	ii
List of Tables . . . . .	iv
List of Symbols . . . . .	v
I. Introduction . . . . .	1
II. Previous Work . . . . .	2
(i) Types of sand movement by wind . . . . .	3
(ii) Mechanism, equations and measurements on the rate of transport . . . . .	4
(iii) Shear stresses at the surface (surface drag) . . . . .	7
(iv) Velocity Distribution over a drifting sand surface . . . . .	8
III. Discussion of the Previous work and Statement of the Problem . . . . .	9
(i) General remarks on Bagnold and Kawamura Equations . . . . .	9
(ii) The problem . . . . .	12
IV. Hydrodynamic effect of the flow on sediment particles . . . . .	13
(i) Theories of sediment transport in rivers . . . . .	13
(ii) Comparison between air and water transport . . . . .	15
(iii) The interaction between flow and bed particles . . . . .	17
(a) Effect of turbulence . . . . .	19
(b) Hidding effect . . . . .	21
(c) Disturbance effect caused by the falling grains . . . . .	21
V. The Sediment Load Equation . . . . .	26

	<u>Page</u>
VI. Determination of $A_*$ and $B_*$ . . . . .	29
VII. Determination of the Correction I . . . . .	30
VIII. Combining the Einstein Correction $\xi$ with the Disturbance Correction . . . . .	33
IX. Experimental Verification using a relatively coarse sand . . .	36
1) Scope and purpose . . . . .	36
2) Test Series (a) . . . . .	36
(i) Experimental Apparatus and Procedure . . . . .	36
(ii) Experimental Results and Discussions . . . . .	38
3) Test Series (b) . . . . .	41
(i) Experimental Apparatus and Procedure . . . . .	42
(ii) Experimental Results and Discussions . . . . .	43
X. Practical Application of the Method . . . . .	44
XI. Summary and Conclusions . . . . .	48
XII. Acknowledgement . . . . .	50
XIII. References . . . . .	51
XIIII. Figures . . . . .	55
XV. Tables . . . . .	76

### ABSTRACT

This study is concerned with the mechanism of sand movement by wind. A method for calculating the rate of transport was developed. This method was based on experience gained in the field of sediment motion in rivers and all available field and wind tunnel data on the subject.

It has been found that the basic forces causing the sediment motion are those of the average lift  $\bar{L}$  and the fluctuating part  $L'$  caused by the turbulence.

Another factor contributing to the motion in the case of wind is the effect of impact, caused by the particle in saltation, in disturbing the bed surface. The effect of impact was found to be a function of the main forces causing the motion and therefore it was introduced as a correction for the mean lift force caused by the distortion of the fluid field around the bed particles.

It has been found that the basic principles governing the rate of sediment transport by water and air are the same. The only difference was found to be the effect of saltation on disturbing the bed surface in the case of air.

The results of this study are represented as a theoretical relation between the flow intensity and the intensity of sediment load. The effect of particle hiding in the laminar sub-layer was combined with the impact correction to give a final wind correction which proved to be a function of the parameter describing the ratio between the submerged weight of the particle and the mean lift force. The method is applicable for calculating the rate of sand transport under a wide range of wind velocities and for sand sizes ranging from a 0.145 mm to 1.00 mm. Application of the derived method for calculating sand transport by wind from natural beaches is given.

# LIST OF FIGURES

## Figure

1. Some experimental data on sand transport as determined by previous investigators.
- 2-a. Variation of the flow of sand with distance along the tunnel.
- 2-b. Development of turbulence and the boundary layer along the tunnel.
3. Change of rate of transport  $q$  with grain diameter  $D$ .
4. The correction  $\xi$ .
5. Effect of the falling particle on disturbing the bed particles.
6. Exchange of bed particles with particles in motion.
7. Theoretical relation between  $\psi_*$  and  $\phi$ .
8. Relation between the correction  $I$  and  $U_*^{3/2} D$ .
9. Relationship between the wind correction  $\frac{\xi}{I}$  and  $\psi$ .
10. Wind tunnel.
11. Wind tunnel. Building 276 RFS
- 12-a. Air intake and Hopper for sand feeding and pitot tube.
- 12-b. Magnehelic Ellison gages used for velocity measurements.
13. Mechanical analysis of sand D and E.
14. Velocity distribution above sand surface (Sand D).
15. Velocity distribution above sand surface (Sand E).
16. Relationship between  $u'$  and  $y'$  and  $D_{50}$ .
17. Comparison between experimental results and Bagnold formula (Sand D).
18. Comparison between experimental results and Bagnold formula (Sand E).
19. Comparison between experimental results and proposed method.

Figure

20. Relation between threshold shear stress coefficient and Reynolds number (after Shields).
21. The correction  $Y$  for non-uniform sediment (after Einstein).
22. Wind tunnel and lay out for experimental series b.

LIST OF TABLES

1. Characteristics of the available experimental and field data on sand transport by wind.
2. Summary of the available experimental and field data on the rate of transport  $q$  and the shear velocity  $U_*$ .
3. Summary of the available data on the coordinates of the focal point.
4. Calculations for  $\frac{\psi \xi}{I} = \psi_*$  vs.  $\phi$  relation as defined by equation 40.
5. Necessary calculations for the corrections  $\xi$ ,  $I$  and  $\frac{\xi}{I}$ .
6. Experimental results on sand D and E (present study).
7. Determination of  $\psi_*$  and  $\phi$  from experimental data (sand D).
8. Determination of  $\psi_*$  and  $\phi$  to be compared with the theoretical values (sand E).
9. Calculation for sand transport (inland) using the proposed method for Reach 8, Salmon Beach, California.



LIST OF SYMBOLS

$A_1, A_2, A_3, A_4, A_5$ and	Constants
$A_*$	Universal constant to be determined experimentally
$B_1$	Impact coefficient
$B_*$	Constant determined experimentally
$C$	Rate of increase of velocity with log height
$C_1$	Constant
$C_L$	Coefficient of lift
$C_B$	Constant in Bagnold's formula
$C_z$	Constant in Zingg's formula
$D$	Grain size of sand particle
$D_{50}$	Mean grain size of sand particle
$D_1$	Grain size of standard sand where $D_1 = 0.25$ mm (Bagnold)
$F$	Force due to impact
$G$	Rate of sand movement as defined by O'Brien and Rindlaub
$G_F$	Rate of sand deposition per unit time and area
$G_s$	Rate of sand scouring from the surface per unit of time and area.
$g$	Acceleration due to gravity
$I$	Impact correction for the equation of sediment motion
$K$	Von Karman constant
$K_1, K_2$ and $K_3$	Constants

$K_k$	Constant in Kawamura formula
$K_s$	Surface roughness = $D_{50}$
$L = \bar{L} + L'$	Lift force total
$\bar{L}$	Average lift force
$L'$	Lift force due to turbulence
$\frac{L'}{\bar{L} \eta_0}$	Standard normal variable
$\ell$	Average travel distance of sand particle
$\ell_r$	Length perpendicular to wind direction and along which the wind is operating.
$m$	Mass of a sand particle
$N$	Number of particles of size $D$ per unit area of bed surface
$O$	Subscript
$P$	Probability of the lift force exceeding submerged weight of sand particle
$\Delta p$	Pressure
$q$	Rate of sand movement per unit width and unit time
$t$	Exchange time, i.e., time required for replacing bed particle by particle in motion
$V_s$	Settling velocity
$U$	Wind velocity
$U_5, U_{18}$	Wind velocity 5 ft. and 18 ft. above the sand surface respectively.
$U_*$	Shear velocity
$U_{*t}$	Threshold shear velocity

$u'$	Coordinate of the focal point (motion)
$X$	Characteristic grain size = $1.39 \delta$ for smooth surface
$Y$	Correction for the lift force due to sediment mixture
$y$	Elevation above the sand surface
$y_o$	Coordinate of the focal point (no motion)
$W_b$	Submerged weight of sand particle
$W_1, W_2$	Initial and final vertical velocities of a sand particle in motion
$Z$	Variable of integration
$Z_o$	Distance from the bed = $0.35 D$
$\alpha$	Dimensionless number = $\left( \frac{\rho_f}{\rho_s - \rho_f} \right) \frac{U_*^2}{g D}$
$\gamma_s$	Dry unit weight of bed material
$\gamma_f$	Unit weight of fluid
$\delta$	Thickness of the laminar sublayer
$\eta_o$	Normalized standard deviation of the turbulent lift force
$\lambda$	Constant
$\nu$	Kinematic viscosity of the fluid
$\sigma, \sigma_1$	Standard deviations
$\xi$	Hidding factor of grains
$\frac{\xi}{I}$	Correction factor for the lift force (wind correction)
$\Delta$	Apparent roughness diameter
$\rho_s, \rho_f$	Density of solid particles and of fluid respectively

$\tau_o$ 

Shear stress

 $\Phi$ Dimensionless parameter expressing the sediment  
load intensity $\psi_*$ Flow intensity =  $\frac{\psi_* Y}{I}$  $\psi$ Dimensionless parameter =  $\frac{Wb}{\bar{L}}$  $\frac{\xi}{I}$ Correction factor for the lift force (wind  
correction)

## I. INTRODUCTION

The problems of supply and loss of sediment at a shore line are of considerable importance along the coast line. One basic mechanism involved in this overall problem is the transportation of sand by wind action<sup>(25)\*</sup>. Many research workers have studied this subject in the laboratory and/or in the field, but the mechanism of the sand movement by wind as yet has not been solved completely. One of the principal difficulties is that the forces acting on a bed particle vary with respect to the orientation of the particle in the bed and the different stages of the motion. Particles in a certain size in a mixture are not subjected to the same flow velocities as they are in the case where the entire bed is composed of material of its own size. Also, particles hidden in the laminar sublayer are not affected by the same forces as those subjected directly to the main turbulent flow. Most of these difficulties were overcome in the case of sediment motion of bottom material in rivers after extensive studies. In 1950 a complete theory was presented by Einstein<sup>(1)</sup> which permitted the calculation of the equilibrium rate at which various discharges will transport the various grain sizes of the bed material in a given channel. Unfortunately, in moving from a sand-water system to a sand-air system, with an enormous difference in density between air and water, the disturbance of the bed particles caused by the falling grains can not be neglected as it is the case for transport by flowing water. It is, however, believed that the basic principles governing the motion in both cases should be the same.

---

\*See references page 51.

With the recognition of the effect of the falling grains in disturbing the bed particles by their impact, especially at low transport rates, a method was developed to describe the mechanism of sand movement by wind. This method is based on the Einstein theory for sand transport by flowing water and all available experimental and field data on the subject of sand movement by wind.

It has been found that the effect of surface disturbance caused by the falling grains can be introduced as a correction for the basic forces causing the motion.

It has been also found that if the Einstein correction,  $\xi$ , for particles hidden between larger particles or in the laminar sub-layer, is combined with the impact correction, a final correction for the case of the sand transport by wind was obtained. This combined correction proved to be a function of the parameter  $\psi$ , which is the ratio of the submerged weight of the particle and the mean lift force caused by the fluid.

An outline of using the proposed method for calculating the transport rate is given. The application of the method was checked for a relatively coarse sand for which suspension can be neglected.

Summary and discussion of the available methods for calculating the rate of sand transport by wind are presented next.

## II. PREVIOUS WORK

The following portion of this study deals mainly with the existing literature on the subject of sand transport by wind. Information on the mechanism of transport will be presented as given by the various authors.

Discussions will be presented in the following part of this study ("statement of the problem").

(i) Types of sand movement by wind (after Bagnold)<sup>(2)</sup>.

For values of  $U_*$ , the shear velocity at the surface, above the threshold value  $U_{*t}$ , some particles from the bed surface are put into motion. The greater the value of  $U_*$ , the more particles will be put in motion. Bagnold<sup>(2)</sup> gave three possible methods of movement: saltation, surface creep and suspension.

a) Saltation

Bagnold observations<sup>(2)</sup>, at low transport rates and feeding sand into the wind tunnel at the upwind section, show that the main motion of the grains is in saltation. Particles rise from the bed with negligible forward speed, are accelerated and carried forward a certain distance by the fluid flow, and finally by the action of gravity, they fall back to the bed again.

b) Surface creep

Bagnold described the mode of motion by surface creep as follows: A portion of the energy which saltating grains have gained from the wind is passed on to the grains that are ejected upward to continue the saltation. The bulk of the energy is, however, dissipated in disturbing a large number of surface grains. This energy is ultimately all lost in friction between the surface grains, but the net result of the continued disturbance of the surface is that a slow forward

creep takes place on the part of the grains composing it.

c) Suspension

Most sand grains are too large to be carried in true suspension. But the motion of the smallest sand grain may in high wind approach suspension.

(ii) Mechanism, equations and measurements on the rate of transport.

a) Bagnold<sup>(2,8,11)</sup>

Bagnold's derivation for the rate of sand transport by wind is based on the change of momentum of a saltating particle and a total number of five laboratory measurements on the rate of sand movement by wind. The rate of sand movement per unit width and unit time,  $q$ , is given by

$$q = C_B \sqrt{\frac{D}{D_1}} \cdot \frac{\gamma_f}{g} U_*^3 \quad (1)$$

where  $D_1$  is the grain diameter of a standard 0.25 mm sand,  $D$  is the grain diameter of sand in questions,  $\gamma_f$  is the specific weight of the air,  $U_*$  is the shear velocity and  $C_B$  has the following values:

1.50 for nearly uniform sand

1.80 for naturally graded sand

2.80 for sand with very wide range of grain diameter

The general characteristics of Bagnold experiments are shown in Table 1.

A summary of his measurements using 0.25 mm diameter sand are shown in Table 2.



b) Kawamura<sup>(3)</sup>

Kawamura following the same basic assumptions as Bagnold, but using only the difference between the shear velocity  $U_*$  and the threshold shear velocity  $U_{*t}$ , obtained the following equation,

$$q = K_k \frac{\gamma_f}{g} (U_* + U_{*t})^2 (U_* - U_{*t}) \quad (2)$$

where  $K_k$  is a constant which should be determined experimentally and has been found by Kawamura to be 2.78 for a sand with a diameter of 0.25 mm. Tables 1 and 2 show the summary of Kawamura measurements.

c) Zingg<sup>(5)</sup>

Zingg in his experimental work collected sand at different depths above the bed for a known period of time. From his measurements shown in Tables 1 and 2, for five different grain size sand, Zingg obtained the following empirical equation

$$q = C_z \left(\frac{D}{D_1}\right)^{3/4} \cdot \frac{\gamma_f}{g} \cdot (U_*)^{3/2} \quad (3)$$

with  $C_z = 0.83$ .

d) O'Brien and Rindlaub<sup>(12)</sup>

These investigators performed a series of field measurement for sand drift by wind at Clatsop Beach near the mouth of the Columbia River in Oregon. Wind velocities were measured at elevations between 0.25 and 12 feet above the ground. The rate of sand movement was related to the wind velocity 5 feet above the sand surface. The predominant sand size

was very nearly 0.008 inch (about 0.194 mm). As a result of these measurements (Table 2), they obtained the following formula.

$$G = 0.36 U_5^3 \quad (\text{for } U_5 > 20 \text{ ft./sec.}) \quad (4)$$

where G is the rate of movement in pounds of dry sand per day passing an imaginary line 1 ft. in length drawn perpendicular to the wind.

e) Experimental studies at the University of California, Berkeley<sup>(4,6)</sup>

Figure 1 shows the experimental results obtained in wind tunnel tests by Bagnold, Kawamura, Zingg and the O'Brien and Rindlaub field measurements upon which equations 1 through 4 were formulated. From Figure 1 it is clear that the sand transport obtained by these different investigators differs widely even though the sand considered has almost the same grain size.

In order to reconcile some of the apparent differences in the various existing relationships for the rate of sand movement, studies with three different grain diameters (Sands A, B and C) were conducted at the University of California, Berkeley.<sup>(4)</sup> The characteristics of these sands and the results are shown in Tables 1 and 2.

From the results of these studies on sand transport the following conclusions were made:<sup>(4)</sup>

- 1) The constant  $K_k$  in equation 2 is not limited in range.
- 2) For sand B it was impossible to find a value for these constants which would permit an adequate description of the experimental data.

3) The Kawamura equation (equation 2) includes the threshold shear velocity,  $U_{*t}$ , which introduces a farther uncertainty in the calculations of transport rates, especially since this is influenced by.

i) personal judgement regarding start of motion

ii) moisture content of the sand

4) The O'Brien and Rindlaub formula (equation 4) should not be used for calculations of transport for any sand diameter except of the size occurring in their measurements.

### iii) Shear stresses at the surface (surface drag)

From the above representations, the importance of the shear velocity  $U_*$  at the bed becomes clear. The value of  $U_*$  is determined by measuring the velocity gradient of the wind near the bed. For a turbulent, steady, uniform flow of fluid over a stable, rough surface, the velocity profile can be represented by the prandtl formula.

$$U = C \log_{10} \frac{y}{y_0} \quad (5)$$

where  $C$  is the rate of increase of velocity with log-height,  $U$  is the wind velocity at elevation  $y$  above the bed and  $y_0$  is a surface parameter characterizing the surface roughness; its value was found by Bagnold to be  $D/30$  or  $0.033D$ .

Under steady flow conditions over flat surfaces,  $U_*$  which is equal to the square root of the shear stress,  $\tau_0$ , at the bed divided by mass density of the fluid,  $\rho_f$ , has a very important physical importance.  $U_*$  is directly

proportional to the rate of wind speed with log-height, and according to Von Karman<sup>(16)</sup>, the constant of proportionality is  $\frac{2.3}{K}$ , where K is a universal constant is equal to 0.4 for conditions of no sediment motion. Equation 5 can be written now in the form

$$U = 5.75 U_* \log_{10} \frac{y}{y_0} \quad (6)$$

iv) Velocity distribution over a drifting sand surface

Once the wind velocity is high enough to move sand particles, the wind velocity distribution is slightly altered by the sand movement. Plotted on semi-log paper, the velocity distributions remain straight lines, but as shown by Bagnold<sup>(2)</sup>, they all seem to meet at a certain point, which he calls a "focus". Bagnold gave the velocity distribution above a surface with sand movement by the equation

$$U = \frac{2.3}{K} U_* \log_{10} \frac{y}{y'} + u' \quad (7)$$

where  $u'$  and  $y'$  are the coordinates of the focal point for drifting surfaces.

Zingg's experiments with five different sizes of sand<sup>(5)</sup> showed that the projected focal points ( $u'$ ,  $y'$ ) appear to bear a relation to grain size in the form,

$$y' = 10 D \text{ (mm)} \quad \text{in mm.} \quad (8)$$

$$\text{and } u' = 20 D \text{ (mm)} \quad \text{in miles/hr.} \quad (9)$$

The range of grain diameters used by Zingg ranged from 0.20 mm to 0.715

mm. His results on 0.505 and 0.715 mm sand were not in agreement with equations 8 and 9.

A summary of all available measurements on the coordinates of the focal point are shown in Table 3.

Zingg's measurements<sup>(5)</sup> showed also that the value of the shear stress at the bed varies from the value obtained indirectly from the velocity profile with  $K = 0.4$ . Zingg proposed a value of 0.375 for  $K$  in equation 7, which is modified now to

$$u = 6.13 U_* \log_{10} \frac{y}{y'} + u' \quad (10)$$

### III. DISCUSSION OF THE PREVIOUS WORK AND STATEMENT OF THE PROBLEM

#### i) General remarks on Bagnold and Kawamura Equations

Although both the Bagnold and Kawamura equations (equations 1 and 2) are the most reliable methods at the present time for calculating the rate of sand movement by wind, they are based on assumptions which are open to question. These assumptions can be summarized as follows:

1 - The effect of turbulence is neglected in the study of sand movement by wind. Bagnold mentioned the following,

"The effect of turbulence is not appreciable until far higher flow values are reached"

He also shows indirectly that the turbulence is greatly responsible for the transportation of bed material by the measurements shown in Figure 2-a

and describing his experimental observations in a special wind tunnel<sup>(8)</sup> as follows:

"Sand placed at the mouth itself was never disturbed even at the highest wind speeds used, despite the fact that the drag and normal velocity gradient must be a maximum here."

The explanation of this is clear, since at the mouth of the wind tunnel, turbulence has not developed. Figure 2-b shows the sketch for the boundary layer and the turbulence development along the wind tunnel. It takes a distance of about 4-5 mt. (Fig. 2-b) for the flow to be fully turbulent. The lack of turbulence at the mouth of the wind tunnel (the first 4-5 mt.) can be the only reason for the failure of sand to move. Since Bagnold has indirectly proved that the average velocity without turbulence is definitely not able to cause the movement, it must be concluded that the turbulence or velocity pulsations are responsible for sand movement by wind. So it is clear now that the sediment movement by wind can not be described by time average values alone, and more understanding of the motion can be obtained only if turbulence is introduced.

2 - Both Bagnold and Kawamura considered an ideal path for the particle, namely, the saltation, for describing the rate of sand transport. A variety of arbitrary assumptions were made concerning the initial and final velocities of the saltating grains.<sup>(2,3)</sup> The rise of the grains from the bed was assumed to be caused by the mechanical impact of the falling grains. This description applies only for low rates of transport. However, at high transport rates the whole description of saltation, for initiating the motion should collapse

since it is only the direct effect of air which puts the material in motion.

Bagnold<sup>(2)</sup> himself mentioned the following description:

"At low wind speeds we undoubtedly have saltation and the effect of grain impact predominating, at higher wind speeds, with an appreciable proportion of the total sand flow moving in suspension and so contributing nothing to the drag, it is possible that the drag due to the remaining saltation is not sufficient to keep the surface wind velocity below the threshold value. In this case the surface wind may set grains in motion by its direct action as it does in water."

Therefore, it is believed that the description of the transport rate based on the effect of saltation only is misleading and should be explained by the variation in the flow conditions at the bed. It is also believed that the effect of saltation especially at low rates of transport should be considered as a factor contributing to the initial disturbance of the bed particle caused mainly by the turbulent fluctuations of the air.

3 - One of the important factors which should be introduced in the study of sediment motion is the grain size of the material. Kawamura ignored this effect completely in his derivation, assuming that the same equation can be used for any grain size. Bagnold assumed that the transport rate appears to vary approximately with the square root of the grain diameter. Reduction of the experimental data obtained at the University of California<sup>(4)</sup>, including the results of the present study, are plotted in Figure 3 which shows a family of curves of different shear velocities  $U_*$ , for the change of the rate of transport with the grain diameter. It is clear from Figure 3 that the Bagnold assumption for the variation of the transport rate,  $q$ , with the square root of the grain diameter (equation 1) is not true. Relations

obtained in Figure 3 are of great importance in understanding the physical phenomena of sediment movement of individual grain sizes as one will see later in this study.

4 - All the available equations on this subject contain a constant. Sediment equations which depend on the value of a constant are not desirable, since this constant usually does not have a physical meaning. Verification of those constants proved that they are not limited in range.

ii) The Problem

To summarize the findings of the above discussions, one will find that:

- 1 - The effect of turbulence should be introduced in the study of sand movement by wind.
- 2 - The effect of saltation should be introduced as a correction for the laws governing the motion and not as the main cause of the transport.
- 3 - The effect of the grain size of the bed particles should be considered as an important factor in any derivation for the sediment equations.
- 4 - The basic pictures of interaction between the fluid and the bed particles was not discussed by any investigator. It is believed that the problem can only be solved if such interaction can be described and understood.

Those are the factors upon which the present research is concentrated.

The problem now is to find a suitable way which describes the overall mechanism of sand movement by wind. In the following parts of this report each phase of the phenomenon will be explained and the desired relationships will be developed.



#### IV. HYDRODYNAMIC EFFECT OF THE FLOW ON SEDIMENT PARTICLES

Numerous studies have been made on the interaction between the fluid flow and the loose material forming the bed of a stream. The results of these studies led to the development of theories describing the phenomenon of sediment transport in a river. One of the most reliable methods is that of Einstein<sup>(1,14,15)</sup>. Since, in both cases of wind and water transport, one will be working with steady, uniform, turbulent flow passing over a granular bed, it is expected that a basic similarity exists between the motion of sediment in rivers and by wind. This, of course does not imply that the laws governing the same phenomena are exactly the same, nor that the theories describing the motion in one case are directly applicable to the other. It is, however, reasonable to assume that some fundamental concepts used in the derivation of one theory may be applied in the derivation of the other. Since it is intended to use in the present study some of the basic principles associated with the motion of sediment by steady streams of water, one could consider it appropriate to give a brief outline of these principles and how one can apply them to the present problem.

##### i) Theories of sediment transport in rivers

In a study of the history of developing the equations and methods by which sediment transport in rivers can be calculated, one will find that it started by some kind of equations similar to those now in use for sand transport by wind. For example, these are the DuBoys<sup>(13)</sup> and others for describing the sediment load in streams. The basic concept regarding the

pattern of motion was that the loose bed is sliding in layers under the action of the flow above. No effect was made in these methods to explain the actual mechanism of interaction between the solid particles and the flow field. General information therefore can not be deduced from these methods and their applications are necessarily limited to particular conditions.

Another way of attacking this problem was to consider the stability of the individual solid particle<sup>(23)</sup>. Unfortunately, these studies did not take into consideration the effect of turbulence. As a result the flow which is responsible for the forces induced on the particle is uniform and steady everywhere on the bed, causing a uniform force field. Therefore, a particle that starts moving at some point of the bed will never have a chance to come back to rest at some other point on the bed, a mode which is inconsistent with the actually observed mode of the motion.

In the last twenty years a new method was developed by Einstein<sup>(1,14,15)</sup>. The basic concept of the Einstein theory for sediment transport in rivers is that at equilibrium there is a continuous exchange, at the same rate, between the particle in motion and the bed. The rate of deposition is found to be a function of the bed load rate, while the rate of removal of grains from the bed is a function of the local flow intensity and the probability of a particle being removed. The functional relationship between the "bed-load rate" in a stream and the flow intensity constitute the "bed-load function" while the equation expressing this relationship is called the "bed-load equation". With the help of this equation it is possible to calculate the

bed-load rate for given flow conditions and bed composition. Einstein extended his work on bed-load rate a step farther to find an expression for the suspended-load. Since true suspension, in sand transport by wind is impossible to occur, in the present study due to the high settling velocities of sand particles, information on suspended-load is not needed. However, since some of the basic principles used by Einstein to develop his bed load-function will be used in the present study, it is considered desirable to give a comparison between wind and water transport.

ii) Comparison between air and water transport

From the above general description of the Einstein bed load function one may ask the question, could it be used for describing the motion of sand under wind action? Before attempting to answer this question, one should consider the principles used in the description of sediment transport which led to the final bed load equation and how they can be applied to the present problem. One should also consider the enormous difference in density between air and water in making the comparison between the eolian and aquatic transport.

Some of the principles and assumptions used in the Einstein theory are<sup>(1)</sup>

- 1) The turbulent fluctuations of velocity and pressure are equally important in predicting sediment motion as the average value of the main flow.
- 2) The "bed-load" transport directly depends on the granular material and on the flow pattern.
- 3) The motion of bed particles by saltation as described by Bagnold<sup>(2)</sup> may be neglected in water.

4) The disturbance of the bed surface by moving sediment particles may be neglected in water.

These are some of the important assumptions used by Einstein in deriving his bed-load function. The most important of them is the first one.

The important role played by turbulence in the case of sediment transport by wind has been demonstrated in different parts of this study. Therefore, it is clear now that the principles gained in this regard from water-grain system may be used in the case of air-grain system.

Statements 2 - 4 inclusive, require comments, since movement by saltation and its effect on disturbing the bed particles and the transport can not be neglected in the case of air.

Kalinske<sup>(18)</sup> has shown that the maximum height of particle "bounce" is proportional to the ratio of sand density to the fluid density. Therefore, for equal drag, this rise of grain in the case of water may be of order of  $\frac{1}{800}$  of that in air. Therefore, neglecting the effect of saltation in the case of water is justified, since the particle rise will be in the order of few grain diameters. But in air, on the other hand, particles will rise higher, gain momentum from the moving fluid and reach the bed with such impact that they may cause considerable disturbance to the bed surface.

One can see that the Einstein description of motion in a grain-water system (namely, "the particle moves if the instantaneous hydrodynamic lift force overcomes the particle weight") should be re-examined in the case of grain-air system since it is not only the hydrodynamic force which causes

the particle to move but also the excitation or disturbance of the bed grains caused by the falling particles. This difference should be expected mainly at low transport rates where the effect of saltation in disturbing the bed particles is most effective.

The effect of the falling grains can hardly be explained by a simple equation, since it depends on the orientation of the bed particles, the rise of the falling grains, the flow intensity and many other factors which can not be enumerated. Since these variables can not be measured very well, the effect of falling grains must be determined from their effect on the motion of the bed material. The significance of this last statement will become clear from the following derivations of the sediment transport equation, in the case of wind, based on the Einstein theory for sediment transport in rivers.

iii) The interaction between flow and bed particles

One can simply look at the general problem of sediment transport as a problem of a steady flow over a granular bed. It is a well known fact that distortion of the flow field around a solid particle resting on the bed generates a lift force acting on the particle, even if the latter is well-sheltered within the sublayer. This force will tend to dislocate the particle and move it away from the solid bed. As far as the particle is still in contact with the bed, the lift force is acting only vertically upwards and it can be expressed as

$$\bar{L} = C_L \rho_f \frac{U^2}{2} A_1 D^2 \quad (11)$$

where,  $C_L$  is the lift coefficient,  $u$  is the instantaneous velocity acting at a distance  $y_1$  from the theoretical bed. Einstein and El-Samni<sup>(17)</sup> conducted flume experiments with plastic spherical balls 0.225 feet in diameter placed in a steady stream of water. The theoretical bed has been determined as the reference level from which distance should be taken so that the measured values of the mean velocity would give the best fit to a logarithmic distribution. This best fit was obtained when the theoretical bed was taken at a distance 0.20 D below the top of the spherical particle. The distance  $Z_0$  at which the velocity should be measured in calculating the lift force has been obtained simultaneously with the determination of the lift coefficient,  $C_L$ . The value of the lift coefficient was obtained by measuring the pressure at two places, one at the top of the spheres and the other near their bases. The pressure difference which is a measure of the lift force can be expressed as

$$\Delta P = C_L \rho_f \frac{U^2}{2} \quad (12)$$

They found that  $C_L$  has a constant value of 0.178 for a wide range of flow conditions provided the average velocity was measured at a distance  $Z_0 = 0.35 D$  from the theoretical bed. Since in both cases of water and air one will be dealing with a steady flow of fluid, it would be reasonable to assume that the value of  $C_L$  is about the same for air and water.

Unfortunately the problem is not as simple as mentioned above. Since, superimposed over the above conditions one has the effect of three important factors,

- a) Effect of turbulence
- b) Effect of the degree of sheltering in the laminar sublayer
- c) Effect of bed particle disturbance caused by the falling grains

There are some other factors but of less degree of importance than the above three. Examples of these are the particle shape ripple formation at the surface and the effect of the sorting coefficient of the bed material.

a) Effect of turbulence

In a turbulent flow all the local flow parameters, and consequently the local lift as well, vary rapidly with time. By measuring the instantaneous values of the lift force exerted by a steady stream of water on the plastic spheres mentioned above, El-Samni found that the total lift force  $L = \bar{L} + L'$  behaves like a random variable having a normal distribution with mean  $\bar{L}$  and standard deviation  $\sigma = \bar{L} \eta_o = \frac{\bar{L}}{2.0}$ .

Knowing the distribution of  $\bar{L} + L'$ , one can establish a criterion of stability for a bed particle as follows

$$L = \bar{L} + L' > W_b \quad (13)$$

where  $W_b$  is the submerged weight of the particle. The probability,  $P$ , that a particle resting at a certain location in the bed becomes just ready to move can be obtained as follows:

$$P = P_r [\bar{L} + L' > W_b] \quad (14)$$

$$\text{or } P = P_r \left[ \frac{L'}{\eta_o \bar{L}} > \frac{W_b}{\bar{L} \eta_o} - \frac{1}{\eta_o} \right] \quad (15)$$

Now, using equations 6 and 12 and considering the velocity  $0.35 D$  above the bed, as found by El-Sammi<sup>(17)</sup> the ratio  $\frac{W_b}{\bar{L} \eta_o}$  in equation 15 can be written as

$$\frac{W_b}{\bar{L} \eta_o} = \frac{(\rho_s - \rho_f) g D^3 A_2}{\eta_o \cdot C_L \cdot \rho_f [5.75 U_* \log_{10} 10.5]^2 D^2 - A_1} \quad (16)$$

where  $\rho_s$  and  $\rho_f$  are the mass densities of the sand and air, respectively.

$g$  = the acceleration due to gravity

$A_1$  = shape factor for the grain area

$A_2$  = shape factor for the grain volume

Equation 16 can be written as

$$\frac{W_b}{\bar{L} \eta_o} = \left[ \frac{\rho_s - \rho_f}{\rho_f} \frac{g D}{U_*^2} \right] \left[ \frac{A_2}{\eta_o C_L A_1 5.75^2 (\log_{10} 10.5)^2} \right] \quad (17)$$

$$\text{Let } \psi = \frac{\rho_s - \rho_f}{\rho_f} \frac{g D}{U_*^2} \quad (18)$$

$$\text{and } B_* = \frac{A_2}{\eta_o C_L A_1 (5.75)^2 (\log_{10} 10.5)^2} \quad (19)$$

and since  $\frac{L'}{\bar{L} \eta_o}$  has a normal distribution with mean zero and standard

deviation  $\sigma = 1$ , the probability,  $P$ , in equation 15 can be expressed as

$$P = \frac{1}{\sqrt{2\pi}} \int_{B_* \psi - \frac{1}{\eta_o}}^{\infty} e^{-\frac{z^2}{2}} dz \quad (20)$$

where  $z$  is a variable of integration.



b) Hiding effect

Naturally the smaller the size of the particle,  $D$ , relative to the thickness, of the undisturbed laminar sublayer,  $\delta$ , the less pronounced is the distortion of the fluid field around the particle, and the intensity of the lift force will be reduced. Also when one considers bed particles of different grain sizes, it can be realized that particles of a certain size in a mixture are not subjected to the same flow velocities as they are in the case where the entire bed is composed of material of its own size. This problem was solved by Einstein<sup>(1,15)</sup> who introduced the effect of particle hiding as a correction  $\xi$ , for the lift force in equation 13.  $\xi$  is given as a function of  $\frac{D}{X}$  (Figure 4), where the value of  $X$  was empirically found by Einstein to be  $1.39 \delta$  for a smooth bed and  $0.77 \Delta$  for rough bed, where  $\Delta$  is the apparent roughness parameter. More details about the correction  $\xi$  is presented in reference number 15.

Now equation 20 may be written as:

$$P = \frac{1}{\sqrt{2\pi}} \int_{B_*}^{\infty} \xi - \frac{1}{\eta_0} e^{-\frac{z^2}{2}} dz \quad (21)$$

c) Disturbance effect caused by the falling grains

Recalling the manner by which the Einstein bed-load equations for rivers was derived, it can be seen that two importance assumptions were made, namely,

1. The motion of bed particles by saltation is neglected.
2. The disturbance of the bed surface by the moving sediment particles

also may be neglected in the case of water.

It has been shown in part (ii) of this section that these two assumptions can not be neglected in the case of air grain system. The question then comes up as to what will happen to the lift  $\bar{L}$  or the  $\psi$  value in equation 21 due to the disturbance action caused by the falling grains? Would it be necessary to introduce a correction factor for that effect? The answer to these questions may be found from the following argument.

If one considers a falling grain at the moment it makes contact with the bed particles, it can be visualized that the grain will have an appreciable velocity at the moment it hits the bed. Different cases can be considered as follows:

1. The grain ricochets upwards from a solid particle supported both ways as a particle in position (3) in figure 5. It will rebound with a velocity nearly equal to the initial velocity of impact<sup>(2)</sup>. One can also expect that the particle in position (3) will become more exposed to the flow than before the collision with particle (5). This case is the exceptional one except for small velocities where the efficiency of the collision remains high.
2. The falling grain will help put other grains, not completely supported, in motion by imparting some of its kinetic energy to them making them more exposed to the flow. Examples of these are particles in position 1, 2 and 4 in Figure 5. In the majority of cases the impact efficiency will be relatively low and the grain will actually rebound to only a small height.<sup>(19)</sup>

Consider now particle number 5 (Figure 5) striking the particle in position

2, for example. Particle 2 is already disturbed by the direct action of the wind. It is very difficult to say how the impact will take place between particles 2 and 5, but generally one may consider the particle in position 2 and try to determine an expression for the effect of impact caused by particle 5 on such a particle. We have,

$$\begin{aligned} \text{Force} &= \text{rate of change of momentum} \\ \text{or } F &= m \frac{(W_2 - W_1)}{t} \end{aligned} \quad (22)$$

where

$F$  = the vertical force on particle 2 as the result of a collision with falling particle 5.

$m$  = mass of the particle

$W_1$  = initial velocity of particle 2; assumed = 0

$W_2$  = final velocity of particle 2

$t$  = time during which the change of velocity took place.

$W_2$  has been assumed by Bagrod<sup>(2)</sup> to be equal to  $B_1 U_*$  where  $B_1$  is an impact coefficient and  $U_*$  is the shear velocity. Kawamura<sup>(3)</sup> found that  $W_2 = K_1 (U_* + U_{*t})$  where  $U_{*t}$  is the threshold shear velocity and  $K_1$  is a constant. Thus, it is reasonable to assume that

$$W_2 = C_1 U_* \quad (23)$$

where  $C_1$  is a constant.

$t$  can be looked at as a measure of the time required for the replacement of a

particle that is just being picked up by the flow at a certain spot of the bed (particle 2, Figure 5) by a similar particle that is being brought to rest at the same spot (particle 5, Figure 5). In other words  $t$  is the Einstein exchange time<sup>(1)</sup>, i.e.,  $t$  can be assumed to be proportional to the time necessary for the particle to settle in the fluid through a distance equal to its own size in the fluid at rest. If the settling velocity is denoted by  $V_s$  then one can write

$$t = K_2 \frac{D}{V_s} \quad (24)$$

$$\text{or } t = K_2 \left[ \frac{D \rho_f}{(\rho_s - \rho_f) g} \right]^{\frac{1}{2}} \quad (25)$$

where  $K_2$  is a constant of proportionality and the other terms are as defined before. Now substituting equations 23 and 25 in equation 22, one gets

$$F = \frac{C_1 \cdot A_2 \rho_s D^3 U_*^{\frac{1}{2}}}{K_2 \left( \frac{D \rho_f}{(\rho_s - \rho_f) g} \right)^{\frac{1}{2}}} \quad (26)$$

$$\text{or } F = K_3 \left[ \frac{\rho_s - \rho_f}{\rho_f} \frac{g D}{U_*^2} \right] \left[ \frac{\rho_s^2 \rho_f}{g (\rho_s - \rho_f)} \right]^{1/2} [U_*^3 D^{\frac{3}{2}}] \quad (27)$$

$$\text{where } K_3 = \frac{C_1 A_2}{K_2} = \text{constant}$$

Using equation 18, equation 27 reduces to

$$F = K_3 \psi \left[ \frac{\rho_s^2 \rho_f}{g (\rho_s - \rho_f)} \right]^{1/2} [U_*^3 D^{\frac{3}{2}}] \quad (28)$$

Equation (28) shows the effect of surface disturbance  $F$  to be a function of the flow intensity  $\psi$ , as given by equation 18 and  $(\frac{\rho_s}{\rho_s - \rho_f})^{1/2} (U_*^3 D^{3/2})$ .

Here again the effect of the force  $F$  on the sediment motion may be considered as a rapid increase in the effect of the hydrodynamic forces acting on the bed particles. In other words, this effect may be considered as an increase in the lift coefficient  $C_L$  of equation 11. Therefore, one may introduce it as a correction for the lift force or the  $\psi$  value in equation 21. From equation 28 one would expect that such a correction should be a function of  $(\frac{\rho_s}{\rho_s - \rho_f})^{1/2} (U_*^3 D^{3/2})$ .

If such a correction is called  $I$ , it should be recognized that for the case of a water-grain system, the value of  $I$  will be equal to unity. Since the correction  $I$  is of opposite effect compared with that of the correction  $\xi$  of equation 21, the lift force should be multiplied by  $I$  and equation 21 may take the form

$$P = \frac{1}{\sqrt{2\pi}} \int_0^\infty \frac{B_* \psi \xi}{I} e^{-\frac{z^2}{2}} dz \quad (29)$$

As mentioned before, the only possible way of describing the effect of surface disturbance (correction  $I$ ) is by its effect on the motion of bed material. Therefore, one would depend on experimental measurements to find such a correction as it is seen in part VII of this study.

## V. THE SEDIMENT-LOAD EQUATIONS

After the interaction between the bed particles and the fluid flow has been explained in the previous part it remains to develop a method which describes the final solution to the problem. For this one may use the equilibrium condition of the exchange of bed particles between the grains in motion and the bed. For each unit of time and of bed area the same amount of sand of a given size must be deposited in the bed as are scoured from it.

Now, consider a uniform grain size sand surface of unit width, over which the wind is blowing, as shown in Figure 6. If  $q$  is the rate of sand moving across Section (o) in dry weight of sand during unit time and unit length,  $L$  is the average travel distance of the sand particle of size  $D$  and  $t$  is the time consumed for replacing a particle in the bed by a similar particle in motion, the rate in dry weight of sand falling on a unit area of sand surface per unit time  $G_F$  can be written as

$$G_F = \frac{q}{L} \quad (30)$$

The number  $N$  of particles of size  $D$  per unit area of the bed surface that at any instance becomes free to move, and indeed do move is proportional to the probability  $P$  as defined by equation 14 as well as to the total population of similar particles per unit bed surface, therefore  $N$  can be written as

$$N = \frac{P}{A_1 D^2} \quad (31)$$

where  $A_1$  is a shape factor for the particle area. The rate of sand scouring from the bed in dry weight per unit area and unit time,  $G_s$ , can be expressed as

$$G_s = \frac{P}{A_1 D^2} \frac{\rho_s g A_2 D^3}{t} \quad (32)$$

$$\text{or } G_s = \frac{A_2}{A_1} \frac{P \rho_s g D}{t} \quad (33)$$

where  $A_2$  is a shape factor for particle volume and the other terms are as defined before.

At equilibrium conditions,  $G_F$  should be equal to  $G_s$  and one gets

$$\frac{q}{L} = \frac{A_2}{A_1} \frac{P \rho_s g D}{t} \quad (34)$$

Einstein<sup>(1)</sup> gives the average travel distance,  $L$ , by

$$L = \frac{\lambda D}{1-P} \quad (35)$$

where  $\lambda$  is a constant and the other terms are as defined above. Now substituting equations 35 and 24 in equation 34, equation 34 can be written as

$$\frac{P}{1-P} = \left( \frac{A_1 K_2}{A_2 \lambda} \right) \left[ \frac{q}{\rho_s g} \left( \frac{\rho_f}{\rho_s - \rho_f} \right)^{1/2} \left( \frac{1}{g D^3} \right)^{1/2} \right] \quad (36)$$

Let

$$\phi = \frac{q}{\rho_s g} \left( \frac{\rho_s}{\rho_s - \rho_f} \right)^{1/2} \left( \frac{1}{g D^3} \right)^{1/2} \quad (37)$$

$$\text{and } A_* = \frac{A_1 K_2}{A_2 \lambda} \quad (38)$$

The probability  $P$  can be written as

$$P = \frac{A_* \phi}{1 + A_* \phi} \quad (39)$$

Now, equations (29) and (39) will give the required relationship between the flow intensity  $\frac{\psi \xi}{I}$  and the sand transport rate,  $q$ , as given by the intensity of sediment transport  $\phi$ . Equating equations 29 and 39 gives,

$$\frac{A_* \phi}{1 + A_* \phi} = \frac{1}{\sqrt{2\pi}} \int_0^\infty e^{-\frac{z^2}{2}} dz \quad (40)$$

$$\frac{A_* \phi}{1 + A_* \phi} = \frac{1}{\sqrt{2\pi}} \int_0^\infty e^{-\frac{z^2}{2}} dz$$

This equation is identical with the Einstein equation for a water-grain system, except the correction  $I$  for the wind condition and using uniform sand. The practical application of equation (41) necessitates the determination of the constants  $A_*$  and  $B_*$  and the  $\xi$  and  $I$  values. The procedure used towards this end will be described in the following section.

Now if one defines the flow intensity  $\psi_*$  as

$$\psi_* = \frac{\xi}{I} \psi \quad (41)$$

The final form of equation (40) will be

$$\frac{A_* \phi}{1 + A_* \phi} = \frac{1}{\sqrt{2\pi}} \int_0^\infty e^{-\frac{z^2}{2}} dz \quad (42)$$

$$\frac{A_* \phi}{1 + A_* \phi} = \frac{1}{\sqrt{2\pi}} \int_0^\infty e^{-\frac{z^2}{2}} dz$$



# VI. DETERMINATION OF $A_*$ AND $B_*$

The application of equation 42 becomes easy once the values of  $A_*$  and  $B_*$  are known. One method of obtaining  $A_*$  and  $B_*$  can be described as follows.

Suppose that a rather large set of measurements are available so that another set of  $\psi$  values as defined by equation 18 and  $\phi$  values as defined by equation 37 can be calculated. Suppose farther that those measurements were obtained under conditions where the corrections  $\xi$  and  $I$  of equation 40 are known to be unity where equation 40 takes the form

$$\frac{A_* \phi}{1 + A_* \phi} = \frac{1}{\sqrt{2\pi}} \int_{B_* \psi - \frac{1}{\eta_0}}^{\infty} e^{-\frac{z^2}{2}} dz \quad (43)$$

These are the cases under which the basic Einstein theory for sediment transport was derived.

The  $\xi$  correction is known to be unity if one uses in the above set of measurements uniform sediments and with a grain size coarse enough such that  $D \gg \delta$ . The only case where one will be sure that the correction  $I$  will be unity is the case of a water-grain system where the effect of the disturbance caused by the falling grains is not in existence as described before.

Therefore, one can conclude that the universal constants  $A_*$  and  $B_*$  can be obtained from measurements made on sand transport by flowing water. As a matter of fact they should be the same for air and water transport. Einstein<sup>(1)</sup> using a set of experimental measurements satisfying the conditions mentioned above obtained the following values for  $A_*$  and  $B_*$ .

$$A_* = \frac{1}{0.023} \quad (44) \quad (29)$$

$$B_* = \frac{1}{7}$$

which should be the same for an air-grain system as explained above. The technique used for finding  $A_*$  and  $B_*$  from measurements and the basic theoretical equation is explained elsewhere.<sup>(1,24)</sup>

## VII. DETERMINATION OF THE CORRECTION I

As mentioned before, the best method of finding the correction I is from experimental data. Therefore most of the available wind tunnel data and field measurements on sand transport by wind were considered. Table 1 shows the main characteristics of these measurements and Table 2 shows the experimental results on the rate of sand transport  $q$  and the shear velocity  $U_*$ .

All these data were used in finding the correction I except those of Kawamura<sup>(3)</sup>. The Kawamura experiments were conducted in a wind tunnel of 80 cm height, 150 cm length and 5 cm width. Due to the short length of this tunnel, it is clear that the flow did not have a chance to become fully developed and the shear stress  $\tau_0$  at the bottom varied considerably along this small length. This fact is discussed in more detail in text books on fluid mechanics where the development of the boundary layer along a flat plate is discussed. For this reason the Kawamura data were excluded from this study.

The steps necessary for obtaining the correction I are as follows:

1. Equation 40 was used to calculate  $\phi$  for different  $\frac{\psi \xi}{I}$  values with  $\eta_0 = 0.5$  as found by El-Sammi<sup>(17)</sup>,  $A_* = 43.5$  and  $B_* = 0.143$  as found by Einstein and using the tables for probability integral. Table 4 shows these calculations. Figure 7 shows the plotting of these data.
2. The  $\psi$  value as defined by equation 18 was calculated for all the available data, the shear stress  $U_*$  and the grain diameter were obtained from Table 2. In making these calculations the air density  $\rho_f$  was taken as  $1.22 \times 10^{-3}$  gm/cm<sup>3</sup> (this is for air of medium humidity at 15 °C); the specific gravity of sand was assumed to be 2.65 for all sands considered; the acceleration of gravity,  $g$  was taken as 980 cm/sec;<sup>2</sup> the grain diameter  $D$  was considered as  $D_{50}$ . Table 5 column 3 show those calculated values for  $\psi$ .
3. The intensity of sediment transport  $\phi$  as defined by equation 37 was calculated using the available experimental values on the rate of sand transport  $q$ , and the other terms in equation 37 as given in step 2. The calculated values of  $\phi$  are shown in Table 5, column 4.
4. Now using the theoretical relationship between  $\phi$  and  $\frac{\psi \xi}{I}$  (Figure 7), the values of  $\frac{\psi \xi}{I}$  can be obtained for each corresponding value of  $\phi$  obtained from step 3. Table 5 column 5 shows the values of  $\frac{\psi \xi}{I}$  as obtained from Figure 7.
5. The  $\xi$  values were obtained as follows:
  - a) The value of the thickness of the laminar sub-layer  $\delta$  was calculated using the equation

$$\delta = \frac{11.6 \nu}{U_*} \quad (45)$$

where  $\nu$  is the kinematic viscosity (taken as  $0.147 \text{ cm}^2/\text{sec}$ ) and  $U_*$  is the shear velocity which can be obtained from Table 2.

The calculated values of the thickness of the laminar sub-layer,  $\delta$ , are shown in Table 5, column 6.

b) The values of  $\frac{D_{50}}{\delta}$  were calculated as shown in Table 5, column 7.

c) Since, for most of the measurements, the bed may be assumed closer to smooth than rough (hydraulically), the values of  $X = 1.39 \delta$  can be used for obtaining the  $\xi$  value as recommended by Einstein<sup>(1)</sup>. Therefore, the values of  $\frac{D_{50}}{X}$  are calculated as shown in Table 5, column 8.

d) Now using Figure 4 the values of  $\xi$  were obtained for the different  $\frac{D_{50}}{X}$  values obtained from above. The  $\xi$  values are shown in column 9.

Table 5.

6. Finally the  $I$  value is obtained using the theoretical value of  $\frac{\psi \xi}{I} = \psi_*$ , say, obtained from step 4, the  $\psi$  value as obtained from step 2 and  $\xi$  from step 5 using

$$I = \frac{\psi_*}{\psi \xi} \quad (\text{by definition}) \quad (46)$$

The  $I$  values are shown in Table 5, column 10.

As was mentioned in part IV of this study and from equation 28, the correction  $I$  appears to be a function of  $\left[ \frac{\rho_s^2 \rho_f}{g (\rho_s - \rho_f)} \right]^{1/2} [U_*^3 D^{3/2}]$ .

Since the value of  $\left[ \frac{\rho_s^2 \rho_f}{g (\rho_s - \rho_f)} \right]^{1/2}$  is considered a constant in the present study, the values of  $I$  as obtained above and the corresponding values of  $U_*^3 D^{3/2}$  were plotted in Figure 8. The calculated values of  $U_*^3 D^{3/2}$  for

all the available data are shown in column 11, Table 5. From Figure 8 it can be seen that an inversely linear relation exists between the  $I$  and  $U_*^3 D^{3/2}$ . The data reasonably fall in a straight line with a slope of minus one on a log-log plot and can be represented by the equation

$$I \cdot U_*^3 D^{3/2} = A_3 \quad (47)$$

where  $A_3$  is a constant.

This relation obtained from Figure 8, can be regarded as one of the proofs that the physical picture of the effect of the surface disturbance caused by the falling grains, which has been given in part IV, seems to be physically sound.

#### VIII. COMBINING OF THE EINSTEIN CORRECTION $\xi$ WITH THE DISTURBANCE CORRECTION I

In using the Einstein correction  $\xi$ , (Figure 4) it has been found that most of the available measurements on sand transport by wind had a  $\frac{D}{X}$  value less than unity. Few measurements (sand number 5 and 6, Table 1) had a value of  $\frac{D}{X} > 1$ . For those few measurements it was found that if the Einstein  $\xi$  curve is modified as shown in Figure 4, a better definition of  $I$  curve (Figure 8) was obtained.

As previously defined,  $\xi$  is a "hiding factor" which expresses the sheltering effect of the degree of submergence in the laminar sub-layer. Actually a change in the  $\frac{D}{X} - \xi$  curve can mean something else also. The

nature of the calculation of the curve is such that any and all factors not specifically taken into account in some other manner are lumped together in the one  $\xi$  value.

Therefore one may explain the modification of the  $\frac{D}{X} - \xi$  curve in the present study by some factors, not yet considered, which is operative in the case of sand transport by wind.

Since the  $\frac{D}{X} - \xi$  curve has a slope of 2 on a log-log plot, it can be represented mathematically by the equation

$$\left(\frac{D}{X}\right)^2 \xi = A_4 \quad (48)$$

where  $A_4$  is a constant and  $X = 1.39 \delta$  as given before. Now substituting the value of  $\delta$  as given by equation 45 and considering the kinematic viscosity  $\nu$  as a constant, equation 48 can be written as

$$\xi = \frac{A_5}{U_*^2 D^2} \quad (49)$$

where  $A_5$  is another constant.

Using equations 47 and 49 the combined correction of the lift force in equation (40) can be written as

$$\frac{\xi}{I} = \frac{A_5 U_*^3 D^{3/2}}{U_*^2 D^2 A_3} \quad (50)$$

or 
$$\frac{\xi}{I} = A_6 \frac{U_*}{D^{1/2}} \quad (51)$$

Since  $\left( \frac{\rho_s - \rho_f}{\rho_f} \right)^{1/2}$  was considered as a constant in the present study,

equation 51 can be written as

$$\xi/I = A/7 = A_7 \left[ \frac{\rho_f}{\rho_s - \rho_f} \frac{U_*^2}{g D} \right]^{1/2} = A_7 \psi^{-1/2} \quad (52)$$

where  $A_7$  is a constant and  $\psi$  as defined by equation 18.

Equation 52 states that the final combined correction  $\frac{\xi}{I}$ , which may be called the "wind correction" is nothing more than a function of  $\psi$ .

Table 5, column 12, shows the  $\frac{\xi}{I}$  values, and Figure 9 represents the relationship between the wind correction,  $\frac{\xi}{I}$ , and  $\psi$ . From Figure 9 it can be seen that a linear relation exists between  $\frac{\xi}{I}$  and  $\psi$ . The data reasonably fall on a straight line with a slope of minus 0.6 on log-log paper instead of -0.5 as indicated by equation 52. The difference in the slope can be explained by the scatter of the data. However, one can fit a straight line with slope-minus 0.5 through the data of Figure 9 with a reasonable degree of success.

If one tries now to summarize how the transport rate can be calculated using the above approach, given the wind speed and the grain size of the sand, the following steps may be used:

1. Use equation 7 to find the shear velocity  $U_*$ , i.e.,  $U = 6.13 U_*$   
 $\log_{10} \frac{y}{y'} + u'$
2. Calculate the value of  $\psi$ , using equation 18, i.e.,  $\psi = \frac{\rho_s - \rho_f}{\rho_f} \frac{g D}{U_*^2}$
3. From Figure 9 find the wind correction  $\frac{\xi}{I}$ .
4. Knowing the value of  $\psi$  find  $\phi$  from Figure 7 and then the rate of sand transport  $q$  using equation 37, i.e.,  $\phi = \frac{q}{\rho_s \cdot g} \left( \frac{\rho_f}{\rho_s - \rho_f} \right)^{1/2} \left( \frac{1}{g D^3} \right)^{1/2}$

IX. EXPERIMENTAL VERIFICATION USING A  
RELATIVELY COARSE SAND

1) Scope and purpose

The experimental program consisted of two series of tests designated as series a and b. The main purpose of these tests were as follows:

- a) To obtain experimental measurements on the rate of sand transport,  $q$ , and the corresponding value of the shear velocity,  $U_*$ , using a relatively coarse sediment to test the proposed theory.
- b) To compare the experimental values of the threshold shear velocity  $U_{*t}$ , under conditions where the effect of surface disturbance is eliminated, with the corresponding values for water as obtained by Shields. <sup>(9)</sup>

2) Test series (a)

(i) Experimental Apparatus and Procedure

The experiments were conducted in a wind tunnel located in Building 276 at the Richmond Field Station of the University of California. The tunnel is 4.0 ft. wide, 1.60 ft. high and 100.0 ft. long and is constructed of plywood (Figures 10 and 11). The wind was generated by a suction fan at the exit end. The mean velocity was varied from 20.0 to 70.0 ft./sec. by controlling the fan speed.

Wind velocities were measured using a standard Prandtl type Pitot tube which was attached to a point gage and introduced into the air stream through the top of the wind tunnel. For small wind speeds, the Pitot tube was connected to a Magnehelic gage having a range of one-half inch of water and



graduated into divisions of 0.2 inch. At high wind speeds the Pitot tube was connected to an Ellison type draft gage having a range of one inch of water and graduated into divisions of 0.01 inch. The Magnehelic gage is usually preferable to use than the Ellison type gage because of its more rapid response to pressure change. Figure 12-B shows both the Magnehelic and Ellison type gages used.

Two different coarse sands were used in this series of experiments. The mechanical analyses of these two sands are shown in Figure 13 and their characteristics are as follows:

Sand	Mean grain diameter (mm)	Sorting Coeff.	Grain sizes range (mm)
D	1.00	1.20	0.90 - 1.20
E	0.88	1.41	0.40 - 1.20

The sand was spread over a length of 62.00 feet of the wind tunnel, with a thickness of about two inches. A hopper to feed sand into the wind tunnel automatically was placed near the entrance to the tunnel (Figure 12-A). The rate of sand feed was adjusted to be equal to the rate of sand transport as measured by the sand trap. This trap was 8.0 ft. long and consisted of 18 compartments permanently fixed at the end of the sand bed. In order to eliminate the side wall effects, the rate of sand transport was measured only over a width of 2 ft. in the central part of the wind tunnel. Sand was removed from the compartments at the conclusion of each run with a vacuum cleaner. The time consumed in each run and the weight of sand collected were

recorded. After each run, the sand surface was well mixed to eliminate any effect of sorting and was leveled to be ready for the next run.

ii) Experimental Results and Discussions

Velocity distribution on the sand surface

Vertical wind profiles were measured at a distance of 11 feet upwind from the end of the sand bed as shown in Figure 11. These measurements were made at the center of the wind tunnel. The velocity distributions obtained with different fan currents are shown in Figures 14 and 15 for Sands D and E, respectively. The velocity profiles obey the logarithmic formula above the focal point (Figures 14 and 15). The focal points were located at:

Sand D ( $D_{50} = 1.00$  mm)

$$y' = 0.14 \text{ ft.}$$

$$U' = 32.0 \text{ ft./sec.}$$

These do not agree with the estimate by Zingg's equation, which gives

$$y' = 0.0328 \text{ ft.}$$

$$u' = 29.40 \text{ ft./sec.}$$

Sand E ( $D_{50} = 0.88$  mm)

$$y' = 0.125 \text{ ft.}$$

$$u' = 32.0 \text{ ft./sec.}$$

These values also do not agree with Zingg's estimate. In order to find a better definition for the coordinates of the focal point  $u'$  and  $y'$ , all the available experimental data shown in Table 3 and the data obtained above on Sand D and E are plotted in Figure 16. Figure 16 shows the relation

obtained between the coordinate of the focal points  $u'$  in ft./sec,  $y'$  in feet and the grain diameter  $D_{50}$  in mm. Since there is no logical method for explaining the physical meaning of the focal point with our present knowledge, it is proposed that the relations obtained in Figure 16 may be used to determine  $u'$  and  $y'$  in equation 7 without further discussions.

#### Rate of Sand Transport

The amount of sand caught by the horizontal trap was measured for shear velocities up to 110 cm/sec. The shear velocity,  $U_*$ , was determined by the slope of the velocity distribution in Figures 14 and 15. Table 6 shows the results of this series of experiments using Sands D and E. These data on the shear velocity,  $U_*$ , and the rate of transport,  $q$ , are plotted in Figures 17 and 18. The experimental data are compared with Bagnold, Kawamura, and the proposed method as follows:

#### Sand D ( $D_{50} = 1.00$ mm)

Figure 17 shows a comparison between the experimental data and the Bagnold equation (equation 1) using a value of  $C_B = 1.5$ . No value for the constant  $K_k$  in the Kawamura equation (equation 2) was found to represent the experimental data. Table 7 shows the necessary data for comparison with the proposed method. The  $\psi$  values were calculated from equation 18, the  $\frac{\xi}{I}$  values were obtained from Figure 9, and the  $\phi$  values were calculated from equation 37. Figure 9 shows a comparison between the theoretical and experimental data, the results are in good agreement if one considers the scatter of data shown in Figure 17. So it can be concluded that the proposed method can

be used for a relatively uniform and coarse sand up to 1.00 mm diameter.

Sand E ( $D_{50} = 0.88$  mm)

As shown from the mechanical analysis in Figure 13, Sand E seems to be a naturally graded sand with grain sizes ranging from 0.40 mm to 1.20 mm. Bagnold recommended a value of 1.8 for the constant  $C_B$  in equation 1 for such a sand. Figure 18 shows a comparison between the experimental data and the Bagnold equation. It is obvious from Figure 18 that the Bagnold equation does not agree with the experimental values. Here again no values for the constant  $K_k$  in Kawamura equation were found to express the measured data.

Einstein<sup>(1)</sup> found that in the case of sediment mixtures, like that of Sand E, a correction factor  $Y$  should be introduced to describe the change in the lift coefficient in a mixture and is a function of  $\frac{K_s}{\delta}$  as shown in Figure 21 (or, of the Reynolds number of the flow at the bed surface). The length  $K_s$  is a roughness diameter and  $\delta$  is the thickness of the laminar sub-layer. The correction factor  $Y$  is unity for uniform sediment. Now, introducing the correction  $Y$ , the flow intensity  $\psi_*$  can be written as

$$\psi_* = \frac{\xi \psi}{I} Y \quad (53)$$

Table 8 shows the necessary calculations for Sand E based on the proposed method and introducing the correction  $Y$  as recommended by Einstein<sup>(1)</sup> and using

$$K_s = D_{50}.$$

Figure 9 shows the comparison between the theoretical and the experimental results. It can be seen from Figure 9 that proposed method is applicable for

sand with a wide range of grain sizes if the correction Y is introduced and the whole calculation is based on the mean grain diameter of the sand mixture, i.e.,  $D_{50}$ .

### 3) Test Series (b)

The basic difference between the laws governing the motion in the case of a grain-water system and a grain-air system was found to be the effect of the falling grains as described by the Correction I. If the above statement is true, one would expect that the laws should be exactly the same if the effect of I can be eliminated in the case of sand transport by wind. The only conditions where the effect of the falling grains, in disturbing the bed particles, can be eliminated are those of the start of motion. There is no reason to doubt that the general principles which Shields<sup>(9)</sup> and others have applied to the definition of the condition at which the surface grains begin to be disturbed by the fluid flow applies for all grain-fluid system. But some discrepancies between the air and water cases are rather to be expected because:

1. Effect of falling grains (in the cases of feeding sand at the up-wind section of the tunnel) is not the same.
2. Exact stage at which initial movement may be said to have started is a matter of personal judgment.

Shield's experimental values of the dimensionless function

$$\alpha = \left[ \frac{\rho_s}{\rho_s - \rho_f} \frac{U_*^2}{g D} \right] \quad (54)$$

in terms of the Reynolds number  $\frac{U_* D}{\nu}$  for grains in water are shown in Figure 20. Bagnold<sup>(2)</sup> showed that the corresponding values of  $\alpha$  found for air gave a curve of the same general shape, but the values of  $\alpha$  were reduced compared with the water conditions. In Bagnold's experimental determination of  $\alpha$ , the effect of surface disturbance was included. It is believed that if such effect is eliminated the values of  $\alpha$  for water and air cases should be the same. Therefore the purpose of this investigation is to find the values of  $\alpha$  for an air-grain system under conditions where the surface disturbance can be eliminated and to compare with Shields' curve for a water-grain system.

#### i) Experimental apparatus and procedure

Experiments were conducted in a wind tunnel located in Building 160 at the Richmond Field Station of the University of California. This tunnel is 1 foot wide, 60 feet long, and 1.28 feet high as shown in Figure 22. The channel was constructed of wood, with one side made of plate glass for observation purposes. The wind was generated by a blower at the entrance of the wind tunnel, driven by an A.C. motor. Wind velocities up to 70 ft./sec can be obtained in this wind tunnel. Three different sands were used Sand D, E and Sand B. For each sand the test procedure was as follows:

1. The first 15 feet of the upwind section of the wind tunnel bed was covered by a fixed artificial roughness (Sands D, E and B, respectively). This length was followed by one square foot of the tunnel of loose sand (Figure 22) and another 5 feet of fixed roughness. By such an arrangement one would have a reasonably fully developed turbulent flow over the loose

sand and due to the small area of the loose sand the effect of disturbance caused by any moving sand can be eliminated.

2. The wind velocity profile at which motion of the loose sand started was recorded and the value of the threshold shear velocity was obtained.

3. The value of  $\alpha$  was calculated using equation 54, and the corresponding  $\frac{U_* D}{\nu}$  was calculated for each sand.

### iii) Experimental results and discussions

The results of this series of experiments can be summarized as follows:

Sand	$D_{50}$ (mm)	$U_*$ (For start of motion) (cm/sec)	$\frac{U_* D}{\nu}$	$\alpha$
D	1.00	100.00	68.00	0.0462
E	0.88	90.00	54.00	0.043
B	0.30	44.00	9.00	0.03

These data are plotted in Shields' curve (Figure 20) - where the agreement between the wind experiments, eliminating the disturbing action of the falling grains, and the water experiments as obtained by Shields is clear. The result of this series of experiments proves again that the basic laws governing the sand motion either by wind or by water is the same and the only difference is the effect of the falling grains in the case of wind condition.

## X. PRACTICAL APPLICATION OF THE METHOD

This part further explains the use of the method for calculating the rate of sand movement by wind and the use of the necessary graphs. Sample calculation for sand transport from a beach is also presented.

### a. Application to uniform sediment

1. The wind velocity  $u$  at a height  $y$  above the bed, and the grain diameter of the bed particle is assumed to be known.
2. Using Figure 16 the focal point  $u'$  and  $y'$  can be obtained and from equation 10, the shear velocity  $U_*$  is calculated.
3. The parameter  $\psi$  is calculated from equation 18.
4. Using the parameter  $\psi$  and Figure 9, the wind correction  $\frac{\xi}{I}$  is obtained.
5. Now with the known value of the flow intensity  $\psi_* = \frac{\psi \xi}{I}$  the  $\phi$  value is obtained from Figure 7 and hence the rate of transport  $q$  from equation 37.

### b. Application to sand with a wide range of grain sizes

The same procedure as for uniform sand except in step 5 one should introduce the Einstein correction  $Y$  which can be obtained from Figure 21. In this case the flow intensity  $\psi_*$  will be calculated as

$$\psi_* = \psi\left(\frac{\xi}{I}\right) Y$$

and the whole calculations will be based on the average grain diameter of the bed particles. This is different from the case of grain-water system where one should separate sand into separate size ranges and calculate them individually.



c. Sample calculation for sand transport from a beach

The greatest difficulty in applying the various equations and graphs for sand transport on natural beaches is the basically irregular wind conditions under field conditions. Both wind duration and speed changes from time to time. Each reach of a particular beach generally is different from every other reach (topography and grain size of sand).

Specific procedures and calculations for determining the rate of sand transport inland from a beach by wind were reported by the writer<sup>(7)</sup>. Those calculations, using the Bagnold equation for the rate of the sand movement by wind, were made for Salmon Beach, California.

In this part, application of the outlined method will be made for reach No. 8 (see reference 7) of Salmon Beach, California.

Application of procedure and steps of calculation as applied to Reach No. 8 of Salmon Beach

The steps in calculating sediment movement from any beach using the method developed in the above discussion may be illustrated using Reach No. 8 of Salmon Beach as follows:

Step 1: wind-speed measurements at a known distance above the bed should be obtained and the direction should be recorded. Also information on the duration of this particular wind speed over the period of time for which the amount of transport is to be calculated should be recorded. This information was obtained for Reach No. 8 using Reference 7. For Salmon Beach wind speed measurements were made 18 feet above the sand surface for the period Sept. 1, 1962 to August 31, 1963. Table 9 Column (1) show the wind speed as recorded.

The four possible directions causing inland sand transport at Salmon Beach were N, NW, W and SW and are shown in Table 9. Wind duration per year,  $t$ , and length of reach  $\ell_r$  contributing to inland transport were obtained from Reference 7 and shown in Table 9.

Step 2: Grain size of the sand bed should be obtained. For Reach No. 8 the mean grain diameter is 0.58 mm.

Step 3: Using  $D_{50}$  and Figure 16 the coordinate of the focal point for the velocity profiles can be obtained. For Reach No. 8 these was found to be

$$y' = 0.03 \text{ ft.}$$

$$u' = 18.00 \text{ ft/sec.}$$

Step 4: For each wind speed, the shear velocity  $U_*$  can be obtained using equation 10; namely

$$U = 6.13 U_* \log \frac{y}{y'} + u'$$

The  $U_*$  values for Reach No. 8 are shown in Table 9, column 2, using the above equation.

Step 5: Using equation 18 the  $\psi$  value can be calculated using  $U_*$  as obtained from step 4,  $D_{50}$  as obtained from step 2 and the normal values of  $\rho_s$ ,  $\rho_f$  and  $g$ . The  $\psi$  values for Reach No. 8 are shown in Table 9, column 3.

Step 6: Using Figure 9 and the  $\psi$  value as obtained from step 5, the wind correction  $\frac{\xi}{I}$  can be obtained. This was done for Reach No. 8, and the  $\frac{\xi}{I}$  values are shown in Table 9, column 4.

Step 7: The flow intensity  $\psi_* = \psi \frac{\xi}{I}$  can be calculated from steps 5 and 6.

Table 9, column (5), shows these values for Reach No. 8.

It is clear from equation 42 that for values of  $\psi_* \geq 25$  the corresponding  $\phi$  value will be very small and approaches zero i.e., there is no motion; therefore, one would suggest that the calculation should start from higher wind speeds in opposite manner of that used in Table 9 till a value of  $\psi_* = 25$  is reached. Wind speeds corresponding to  $\psi_* \geq 25$  should not be considered since they contribute nothing to the motion of the bed material. It is believed that this is a very good characteristic of the use of the proposed method since it tells us where the motion starts and where one can stop his calculation. This fact shows how the Bagnold formula is misleading, since it gives an answer to the rate of transport rate for any value of  $U_*$  other than zero.

Step 8: Using  $\psi_*$  values obtained from step 7 the  $\phi$  values can be obtained from Figure 7. Table 9, Column 6 shows those values for Reach No. 8.

Step 9: Using equation 37, namely

$$\phi = \frac{q}{(\rho_s \cdot g)} \left( \frac{\rho_f}{\rho_s - \rho_f} \right)^{1/2} \left( \frac{1}{g D^3} \right)^{1/2}$$

The rate of transport  $q$  can be calculated, since the above equation can be written as

$$q = \phi (\rho_s \cdot g) \left[ \frac{\rho_s - \rho_f}{\rho_f} \right]^{1/2} (g D^3)^{1/2}$$

or for Reach No. 8 and substituting the known values for  $\rho_f$ ,  $\rho_s$ ,  $g$  and  $D$  in gm-cm-sec system, for example,

$$q = 45.30 \phi \quad \text{in gm/cm - sec.}$$

The  $q$  values are shown in Table 9, column 7.

Step 10: Using the information obtained from steps 1 and 9 the total transport rate for each wind direction can be calculated in dry weight of solids, using

$$Q = q \ell_r T$$

where  $\ell_r$  is the length contributing to transport (step 1 and reference 7) in cm, and  $T$  is the wind duration in seconds per year. The values of  $Q$  for Reach No. 8 are shown in Table 9, column 9, for each possible wind direction contributing to inland sand movement.

Step 11: The total annual inland transport  $Q_t$  can be found by adding the total  $Q$  for each wind direction. For Reach No. 8 of Salmon Beach, this was found to be  $2.36 \times 10^6$  lb/year as compared with  $5.40 \times 10^6$  using the Bagnold formula<sup>(7)</sup>. The reason for this big difference is clear from the discussion shown in step 7.

## XI. SUMMARY AND CONCLUSIONS

The present investigation is concerned with the study of the mechanism of sand movement under the wind action. A method for calculating the rate of sand transport was developed. This method was based on the Einstein theory for sediment transport in rivers and all available field and laboratory measurements on the subject of sand movement by wind. The main findings of this study can be summarized as follows:

1. The turbulence or velocity pulsations are largely responsible for sand movement by wind and their effect should be introduced.

2. The description of the transport rate based on the effect of saltation only is misleading and should be explained by the variation in the flow conditions at the bed.
3. The basic forces causing the sediment motion are those of the average lift  $\bar{L}$  and the fluctuating part  $L'$  caused by the turbulence. The effect of saltation, in the case of wind, can be introduced as a correction for those basic forces.
4. Basically the main principles governing the rate of sediment transport by water and air are the same. The only difference appears to be the effect of saltation on disturbing the bed surface in the case of air.
5. The effect of surface disturbance was introduced as a correction,  $I$ , for the main lift forces causing the motion.
6. If the Einstein correction  $\xi$  for particle "hiding" in the laminar sub-layer is combined with the above correction for surface disturbance, a new "wind correction" was obtained which seems to be a function of the parameter  $\psi$  given by equation 18.
7. The conditions of start of sediment motion as given by Shields in the case of water are the same for wind conditions if the effect of surface disturbance is eliminated.
8. Experimental curves were obtained for the coordinate of the focal point  $u'$  and  $y'$  as a function of the grain diameter.
9. The method is applicable for calculating the rate of sand transport under a wide range of wind velocities and for sand sizes ranging from 0.145 mm to 1.00 mm.

10. The derivation of the method is based on uniform sand. It has been found that it can be used for sand with a wide range of grain sizes if the Einstein correction  $Y$  is introduced. Practical application of the method for uniform and non-uniform sand is given together with a sample calculation for sand transport from a beach by wind using the derived method.

## XII. ACKNOWLEDGEMENT

The author wishes to express his gratitude and deep thanks to Professor J. W. Johnson for his valuable discussions, criticisms and guidance. He suggested the subject of the thesis and supervised the work.

Special acknowledgement is due to Professor H. A. Einstein. His enthusiasm, frequent stimulating discussions, comments and suggestions are gratefully acknowledged and sincerely appreciated.

Thanks are also due to Professor D. Blackwell for reading the manuscript.

The author would like to thank Mrs. French for kindly typing the manuscript.

## REFERENCES

XIII. REFERENCES

1. Einstein, H. A., "The bed load function for sediment transportation in open channel flows," U. S. Department of Agriculture Tech. Bull., 1026, 1950.
2. Bagnold, R. A., "The physics of blown sand and desert dunes," William Morrow and Comp., New York, 265 pp.
3. Kawamura, R., "Study on sand movement by wind," Report of the Institute of Science and Technology, University of Tokyo, Vol. 5, No. 3/4, Oct., 1951.
4. Yves-Belly (with Addendum II by Abdel-Latif Kadib), Coastal Engin. Research Cent., U. S. Army, T.M. No. 1, "Sand movement by wind", Jan, 1964.
5. Zingg, A.W., "Wind tunnel studies of the movement of sedimentary material," Proc. of the Fifth Hydraulic Conf., 1952.
6. Horikawa, K., and H. W. Shen, Beach Erosion Board, Tech. Mom. No. 119, "Sand movement by wind", 1961.
7. Kadib, A. A., "Calculation procedure for sand transport by wind on natural beaches," U. S. Army, Coastal Engin. Research Center, Misc., paper No. 2-64, April, 1964.
8. Bagnold, R. A., "The movement of desert sand," Proceeding, Royal Soc., of London, Series A, No. 892, Vol. 157, 1936, pp. 594-620.
9. Shields, A., Mitt. Vers. Anst. Wasserb. u. Schiffb. Berl. Heft 26 (1936).
10. White, C. M., "Equilibrium of grains on bed of streams," Proc. Royal Soc. of London, Vol. 174A, pp. 322-334, 1940.
11. Bagnold, R. A., "The movement of a cohesionless granular bed by fluid flow over it," British Journal of Applied Physics, Vol. 2, No. 2, Feb. 1951.
12. O'Brien, M. P., and Rindlaub, B. D., "The transportation of sand by wind," Civil Engineering, May 1936.
13. Dy Boys, P., "Etudes du Regime du Rhone et l'action Eerecee' par les Laux sur un Lit a Fond de Gravieres Undefinitement Afflouibbable," Annales des Pont et Chausees, Series 5, Vol. 18, pp. 141-195, 1879.



14. Einstein, H. A., "Formulas for the transportation of bed-load," Trans. ASCE Vol. 107, pp. 561-573, 1942.
15. Einstein, H. A., and Ning Chien, "Transport of sediment mixtures with large sizes," I.E.R. University of Calif., MRD Sediment Series No. 2, June 1953.
16. Von Karman, T., "Turbulence and skin friction," Journ. Aero. Science, Vol. 1, Jan. 1934.
17. Einstein, H. A., and El Samni, Elsayed, A., "Hydrodynamic forces on a rough wall," Rev. Mod. Phys. 21: 1949, pp. 520-524.
18. Kalinske, A. A., "Criteria for determining sand-transport by surface creep and saltation," Trans. AGU, pt. 2: 639-643, 1942.
19. Danel, P. and others, "Introduction a l'etude de la saltation," La Houille Blanche, Vol. 8, No. 611953, pp. 815-829.
20. Johnson, J. W., "Sand movement on coastal dunes," University of Calif., Hyd. Engin Lab. Rept. No. (HEL-2-3), Jan. 1963.
21. Ford, E. F., "The transportation of sand by wind," Trans. A.G.U., Vol. 38, No. 2, April 1957.
22. Emmett M. Laursen, "An investigation of the total sediment load," Iowa Inst. of Hydr. Res. State Univ. of Iowa, June 15, 1957.
23. Jeffrey, H. "On the transport of Sediments by Streams", Proc. Cambridge Phil. Soc. Vol. 25, pp. 272-276.
24. G. Kalkanis, Coastal Eng. Research Cent., U. S. Army, T.M. No. 2, "Transportation of bed material due to wave action", Feb., 1964.
25. Johnson, J. W., "The supply and loss of sand to the coast," Jour. Waterways and Harbors Div., Proc. Am. Soc. Civil Engrs. Vol. 85, No. 119, August 1960, 51 p.
26. Bagnold, R. A., "Experimental on a gravity-free dispersion of large solid grains in a Newtonian fluid under shear", Proc. Roy. Soc. A 225, 1954, p. 39-63.
27. Bagnold, R. A., "Some flume experiments on large grains but little denser than the transporting fluid, and their implications", Proc. I. C.E. No. 6041, 1955, p. 174-205.

28. Bird, Warren and Lightfoot, "Transport phenomena", J. Wiley and Sons, 1960.
29. Brown, C., "Sediment transportation", Chapter VI, Engineering Hydraulics by H. Rouse, J. Wiley and Sons, 1950.
30. Carstens, M. R. "Accelerated motion of a spherical particle", Trans. A.G.U. Vol. 33, No. 45, 1952.
31. Chien, Ning "The present status of research on sediment transport" Trans. ASCE, Vol. 121, 1956.
32. Garde, R. J. and M. L. Albertson, "Bed-load transport in aluvial rivers", La Houille blanche, No. 3, 1961.
33. Hinze, J. O. "Turbulence", McGraw-Hill, 1959.
34. Lane, E. W. and A. A. Kalinske "The relation of suspended to bed material in rivers", Trans. A.G.U. 1939.
35. McNiven, J. and P. Lin "Sediment concentration and fall velocity," Proc. Second Midw. Conf. on fluid mechanics, Ohio State Univ. 1952, p. 401-411.
36. Mayer-Peter, E., "Quelques problems concerrants le chariage des matieres solides", etc. La Houille blanche, No. B, 1949.
37. Nizery, A., "Note sur L'entrainement des Materiaux Par charriage" La Houille blanche No. A, 1949.
38. Chepil, W. S. "Dynamics of wind erosion", Soil Science, Vol. 60, Oct., 1945, pp. 305-320, Vol. 60, Nov. 1945, pp. 397-411, Vol. 60, Dec. 1945, pp. 475-480.

XIIII. FIGURES

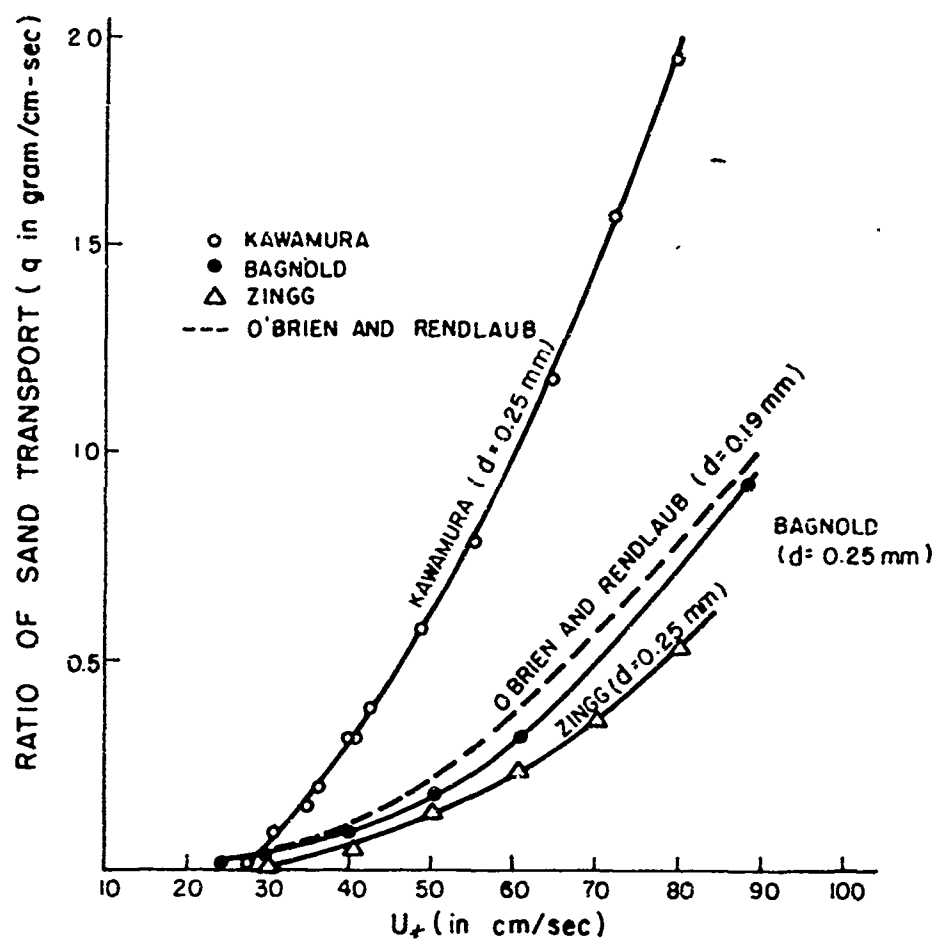
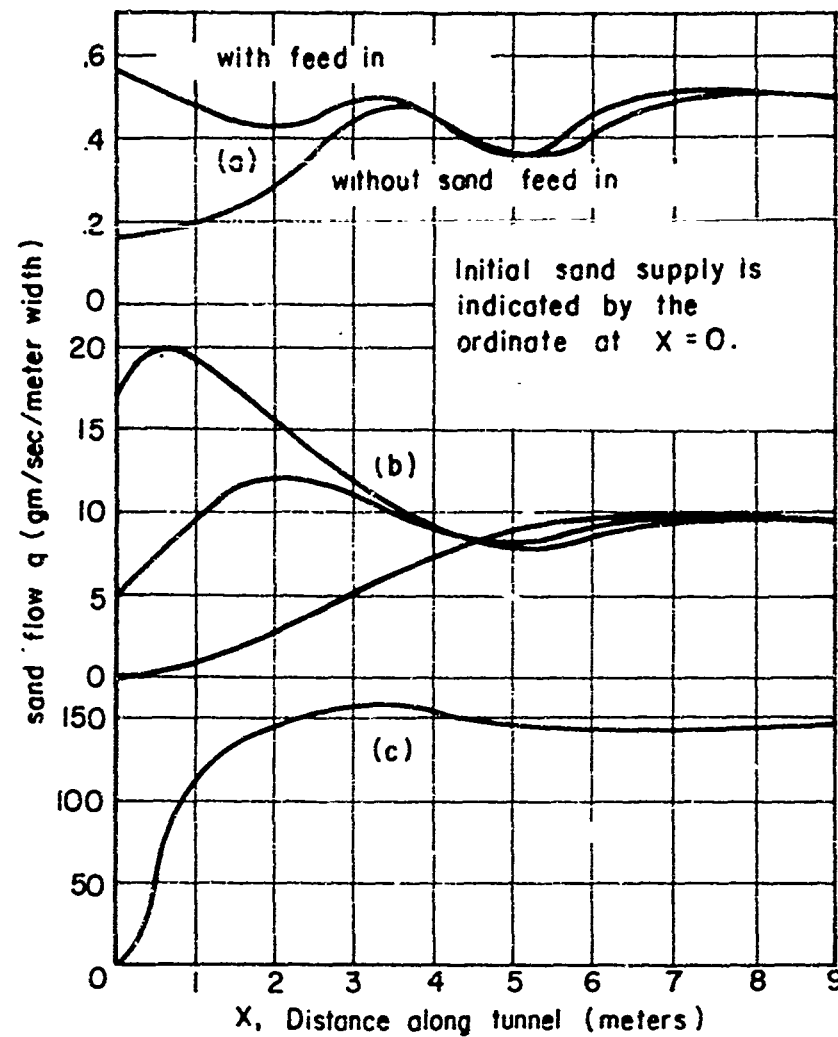
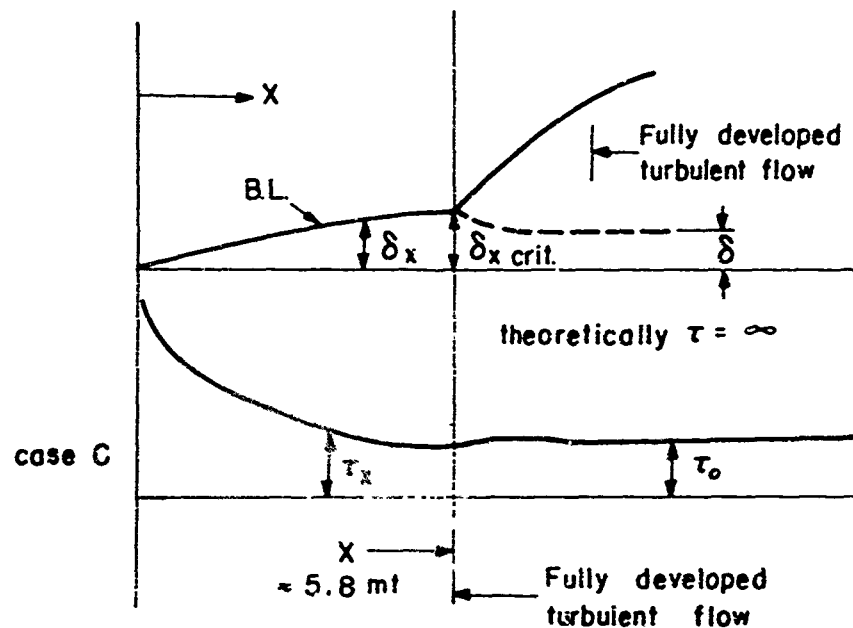


FIG. 1 SOME EXPERIMENTAL AND FIELD DATA ON SAND TRANSPORT AS DETERMINED BY PREVIOUS INVESTIGATORS



(a) mean air speed 430 cm/sec (below threshold)  $V_{*c} = 19.5$ ; (b) mean air speed 490 cm/sec,  $V_{*c} = 36$ ; (c) mean air speed 930 cm/sec,  $V_{*c} = 92$ .

Fig 2a variation of the flow of sand with the distance along the tunnel after Bagnold



$$\text{take } R_x = 400,000$$

$$400,000 = \frac{U_* X}{\nu}$$

case c:

$$\text{assume } U_* = 100 \text{ cm/sec}$$

$$\nu = 0.145 \text{ cm}^2/\text{sec}$$

$$X = \frac{0.145 \times 400,000}{100 \times 100}$$

$$= 5800 \text{ m}$$

Fig. 2b development of turbulence and the boundary layer along the wind tunnel

FIG. 2

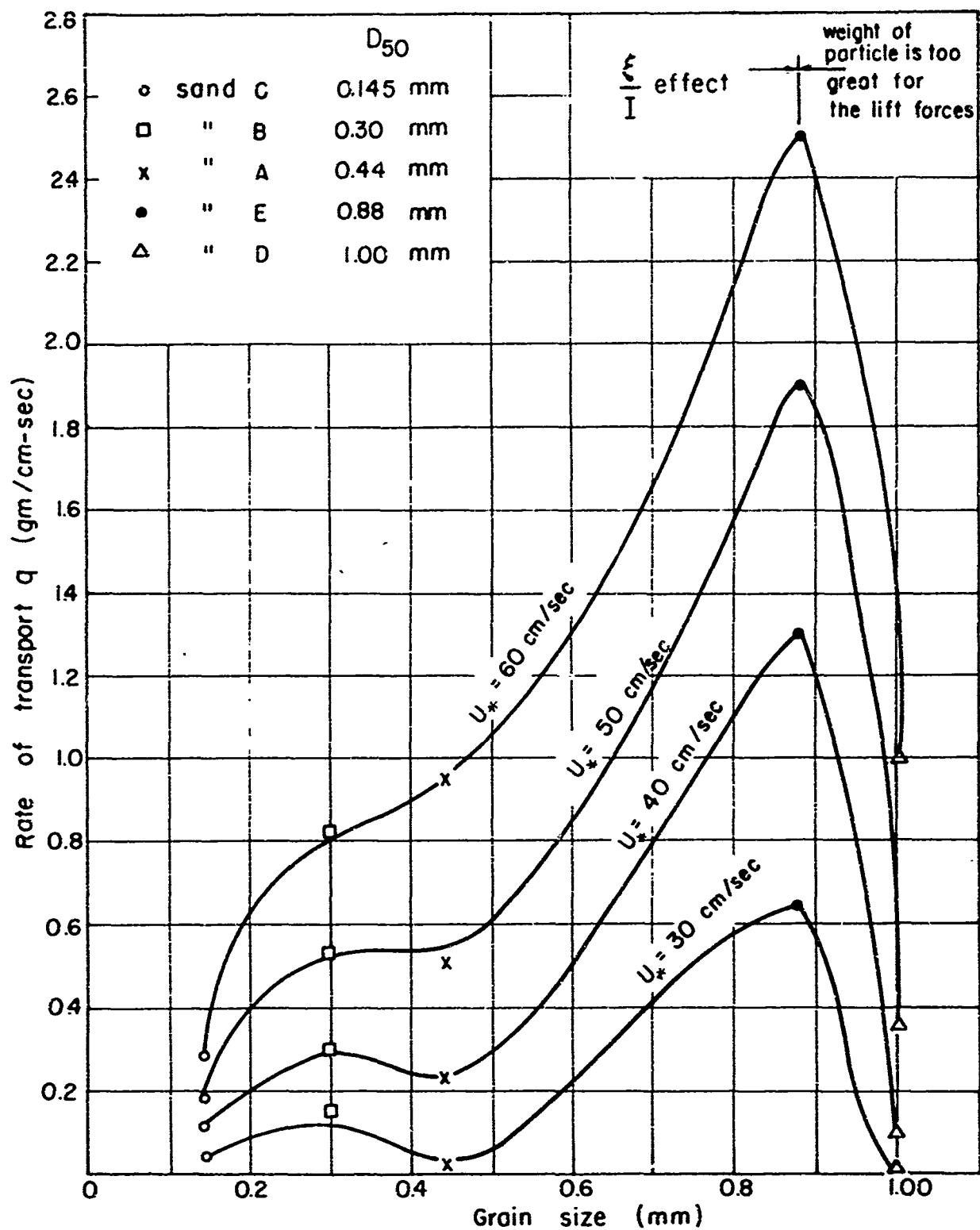
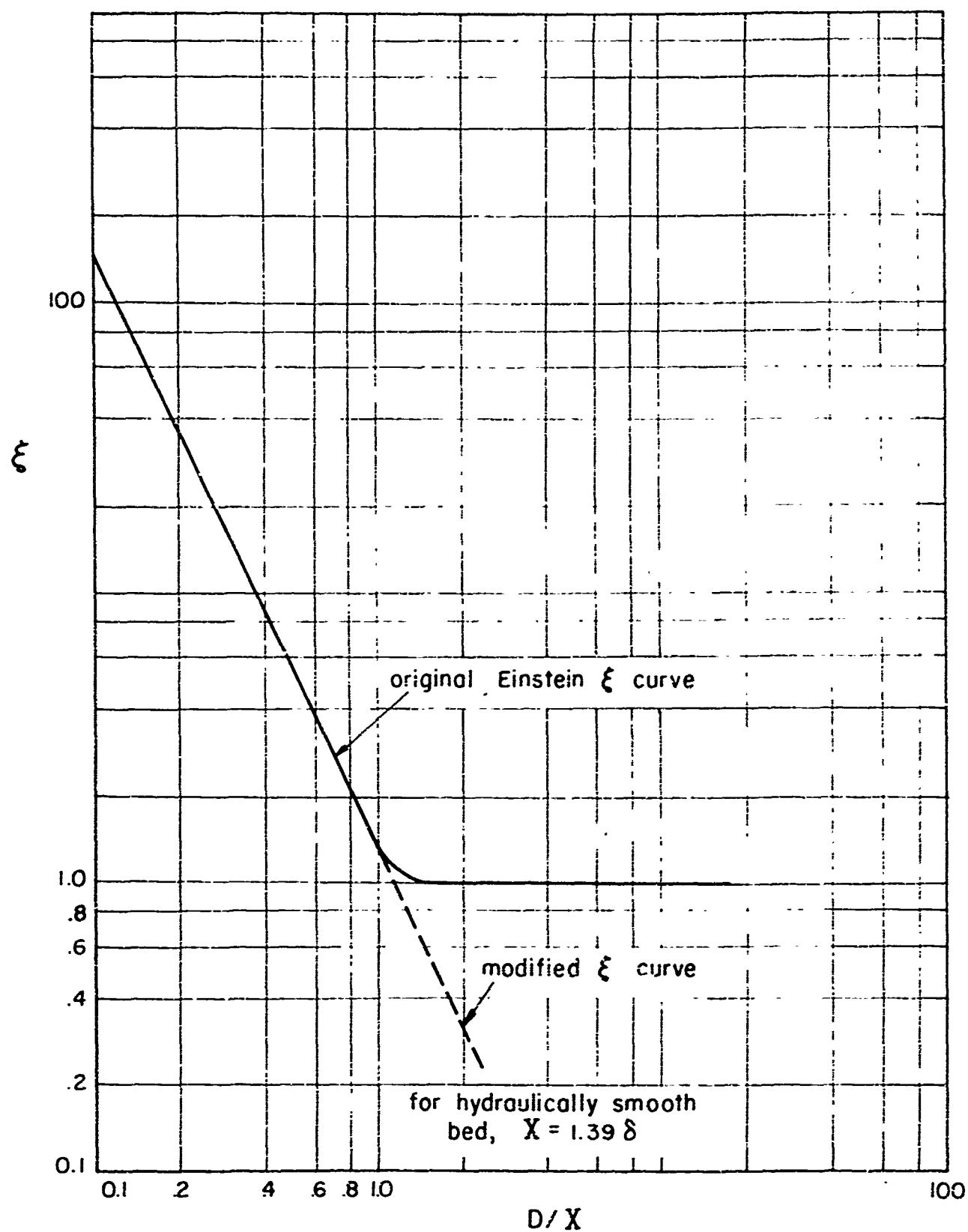


FIG. 3 CHANGE OF TRANSPORT RATE  $q$  WITH GRAIN DIAM.  $D$

FIG. 4 THE CORRECTION  $\xi$

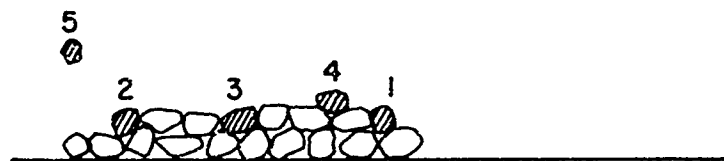


FIG. 5 EFFECT OF FALLING PARTICLE (5) IN DISTURBING THE BED PARTICLES

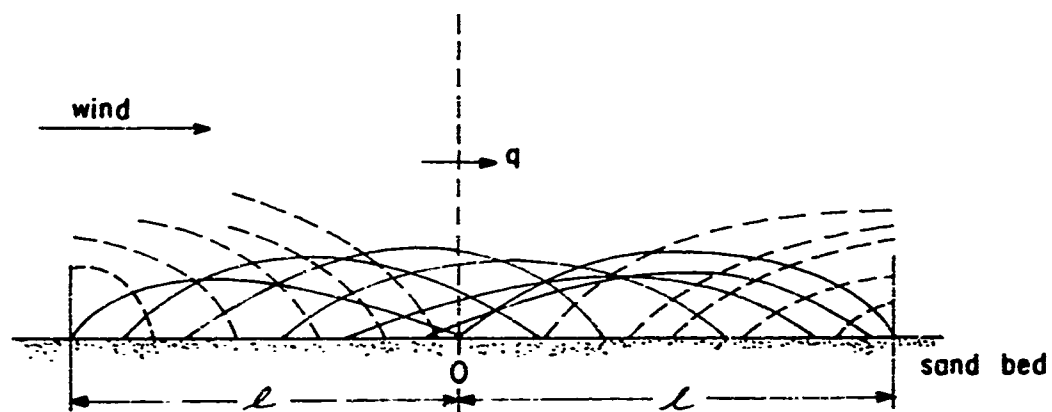


FIG. 6 EXCHANGE OF BED PARTICLES WITH PARTICLES IN MOTION



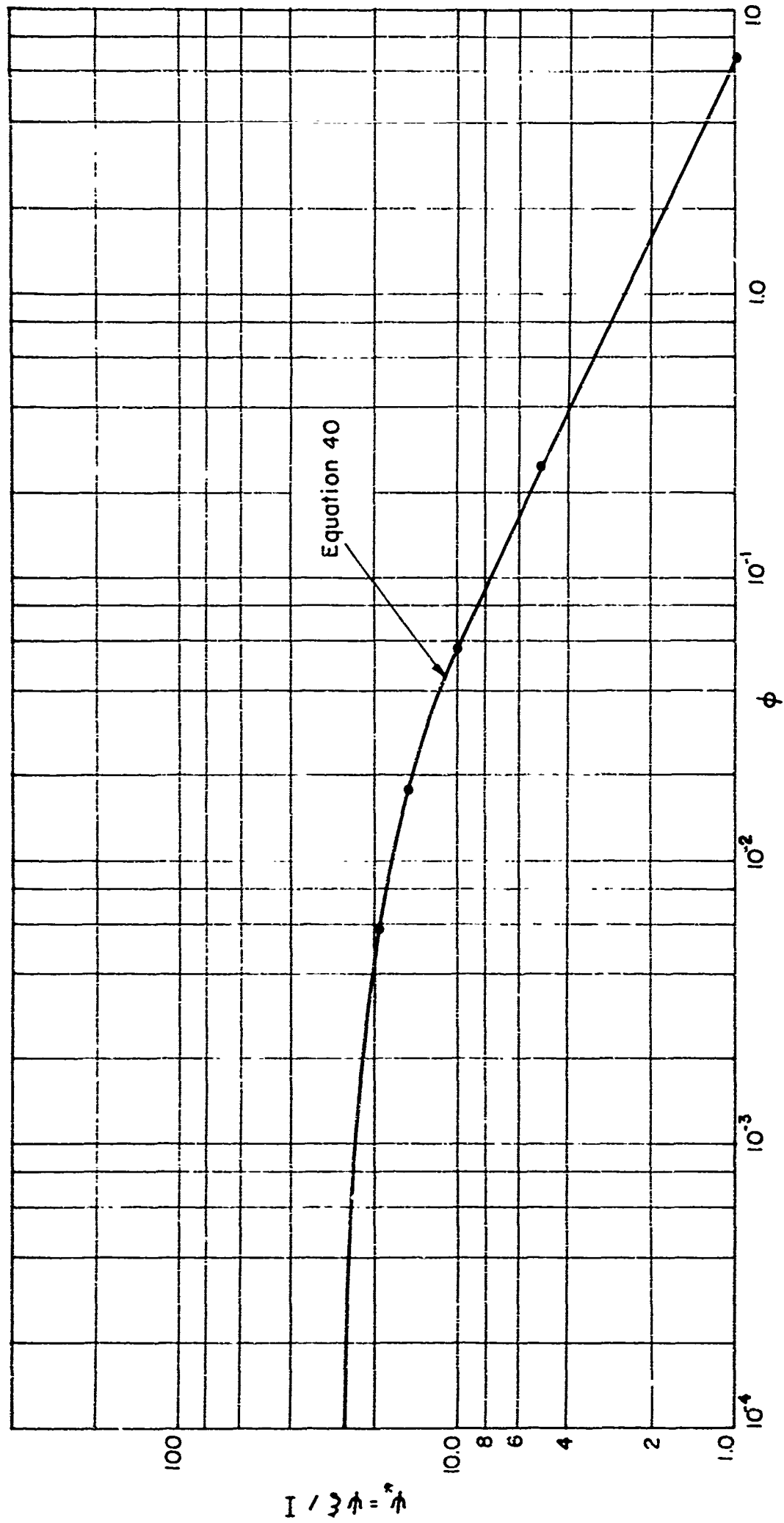


FIG 7 THEORETICAL RELATION BETWEEN THE FLOW INTENSITY  $\psi_*$  AND THE INTENSITY OF SEDIMENT TRANSPORT  $\phi$

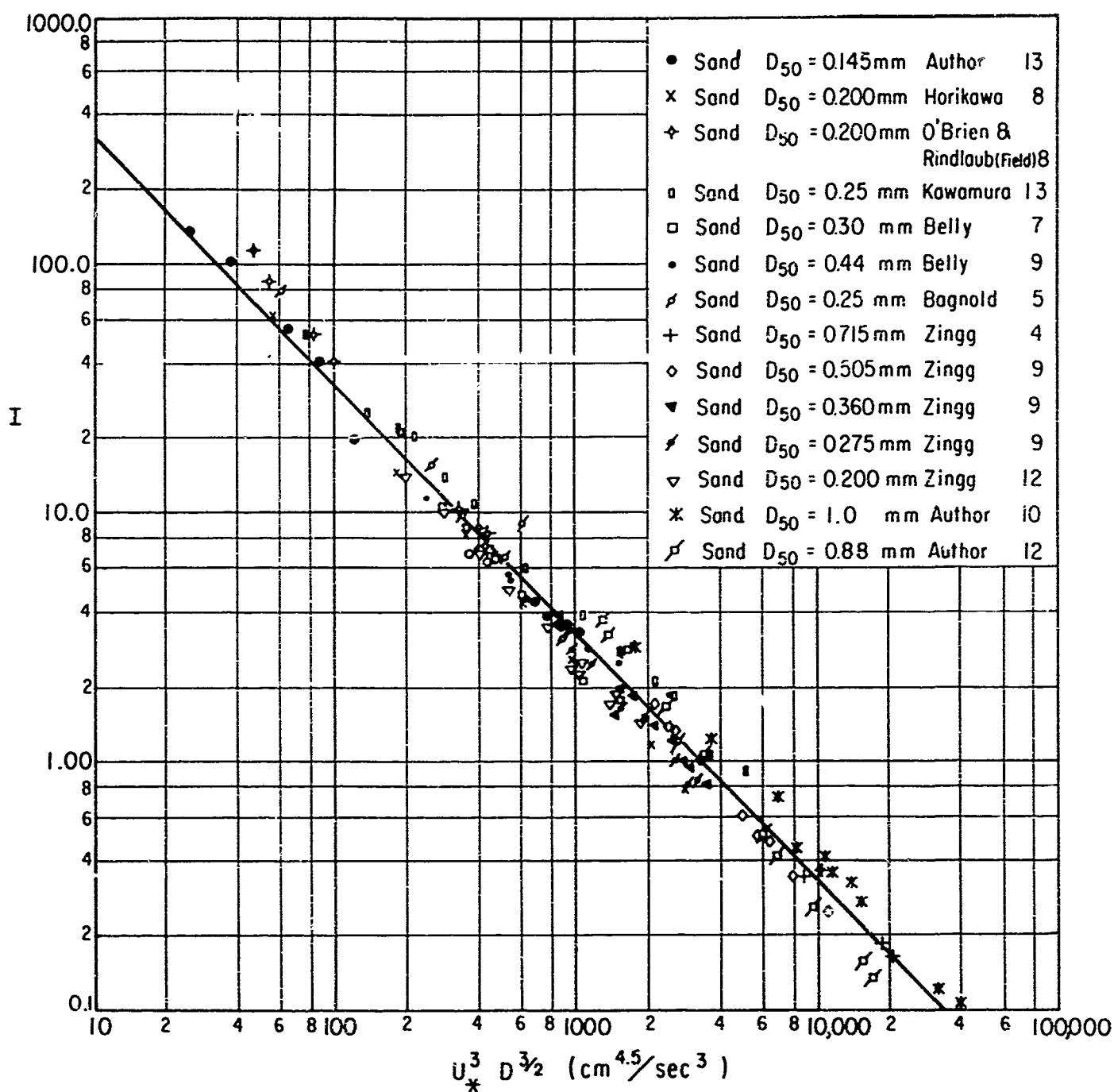


FIG. 8 RELATION BETWEEN THE CORRECTION I AND  $U_*^3 D^{3/2}$

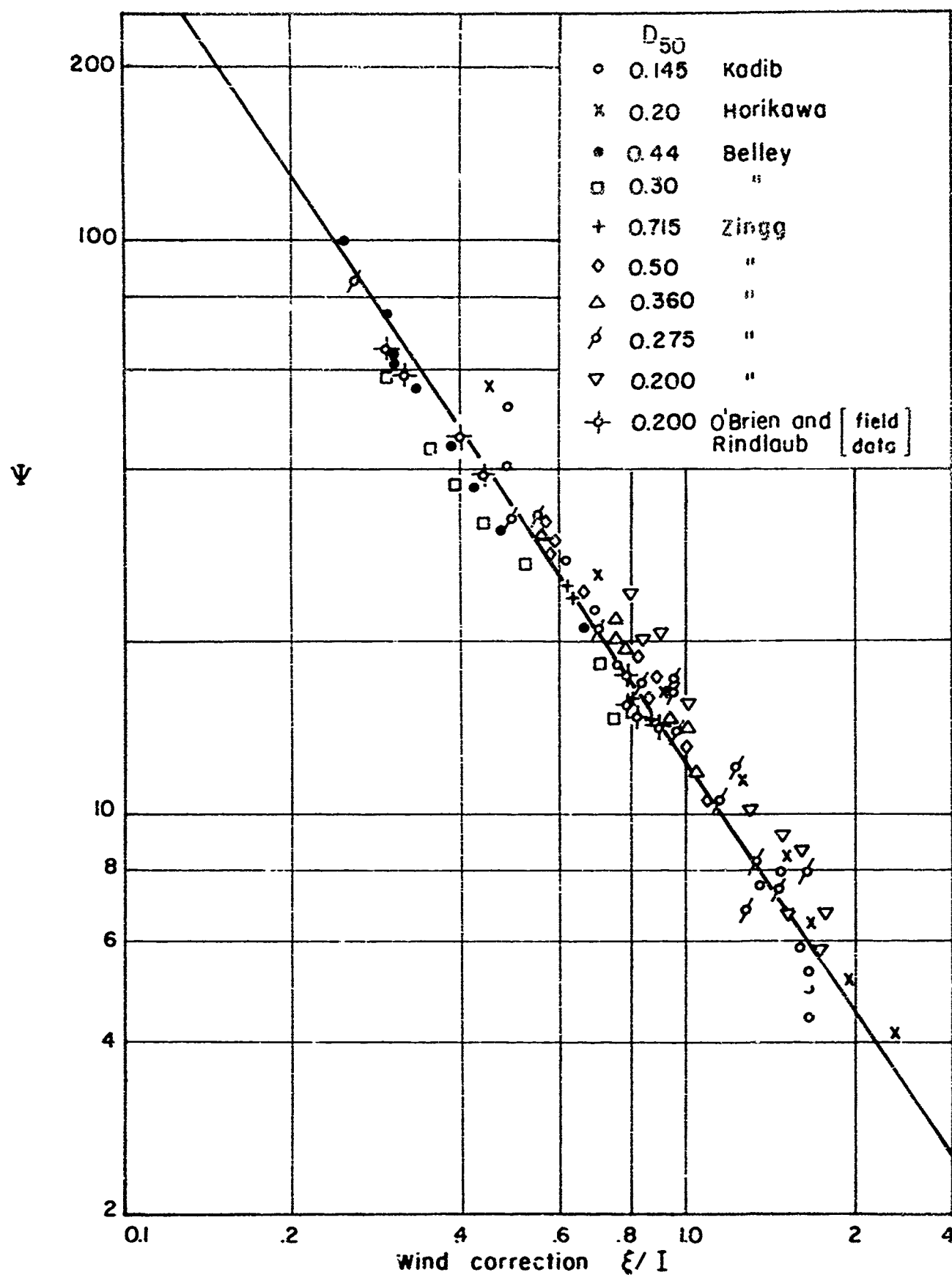


FIG. 9 RELATIONSHIP BETWEEN THE WIND CORRECTION  $\xi/I$  AND  $\Psi$  FOR ALL AVAILABLE DATA ON SAND TRANSPORTATION BY WIND

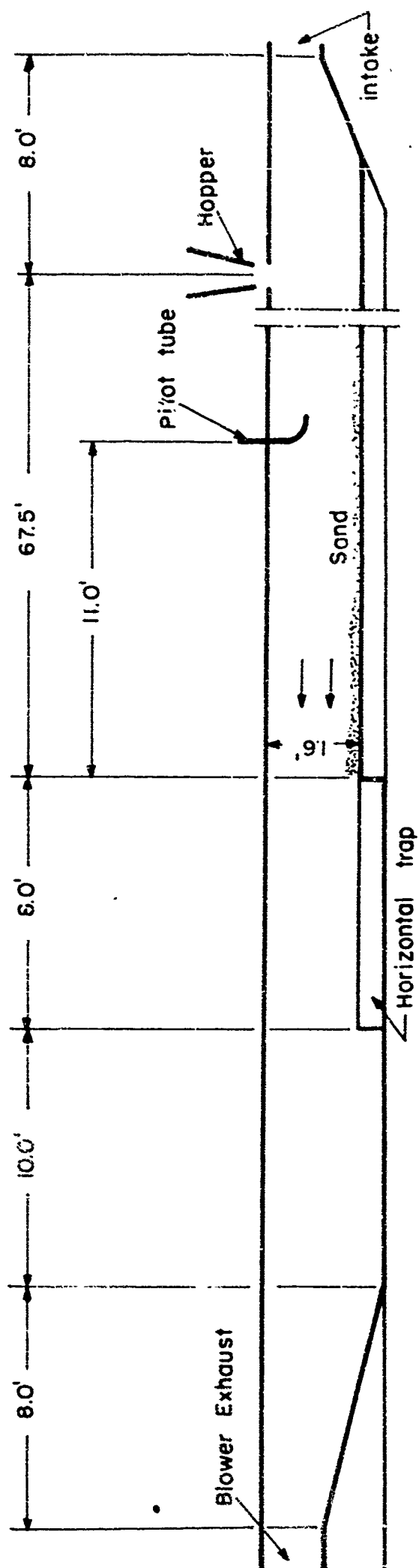
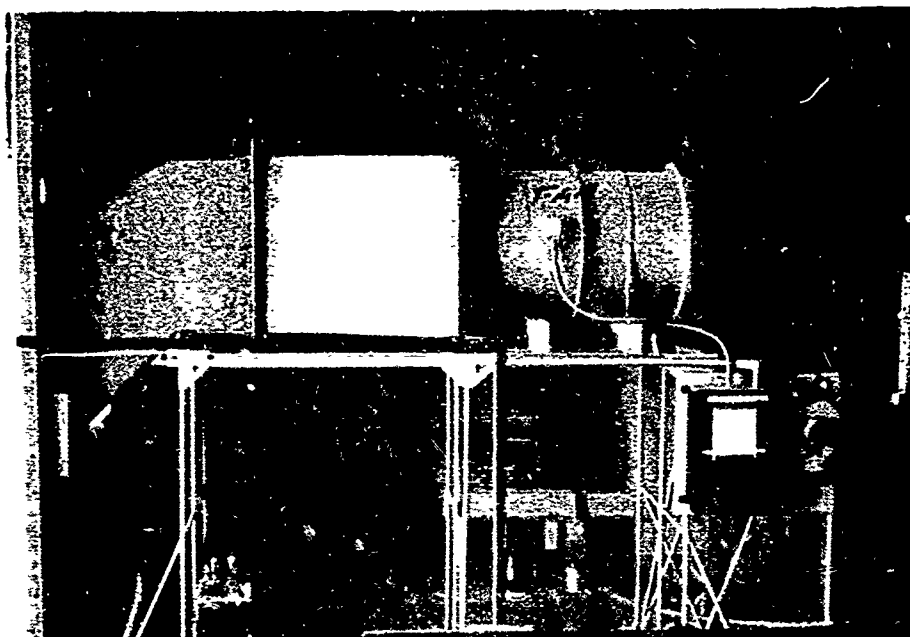


FIG 10 WIND TUNNEL

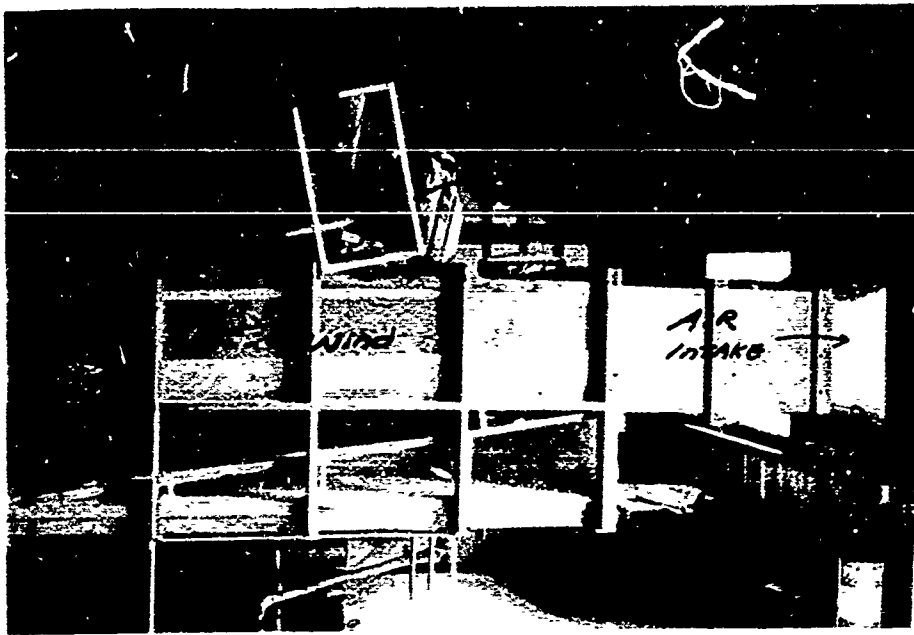


(a)



(b)

FIG. II WIND TUNNEL



66

FIG.12-A AIR INTAKE & HOPPER FOR SAND FEEDING

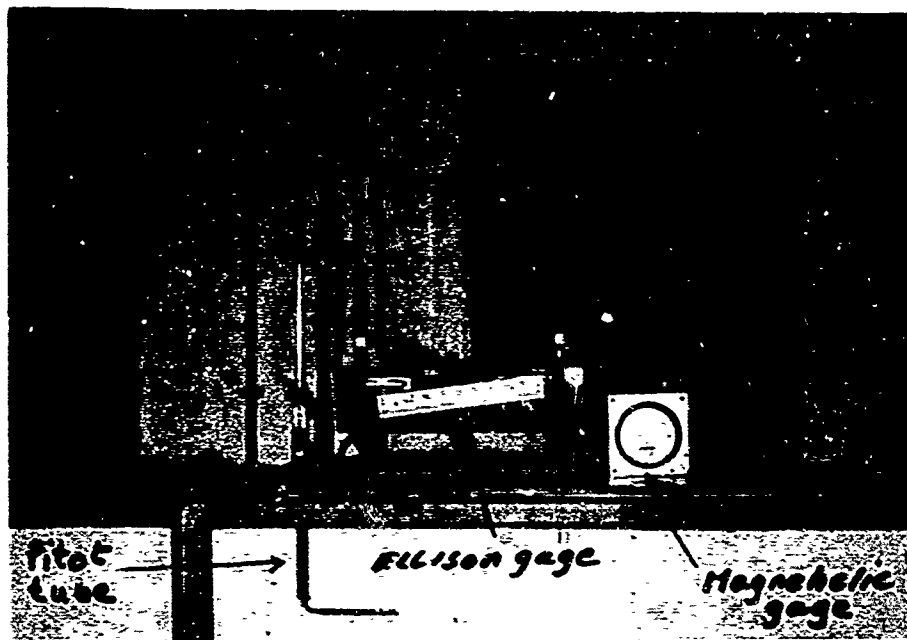


FIG.12-B MAGNETIC ELLISON GAGES AND PITOT  
TUBE FOR VELOCITY MEASUREMENTS

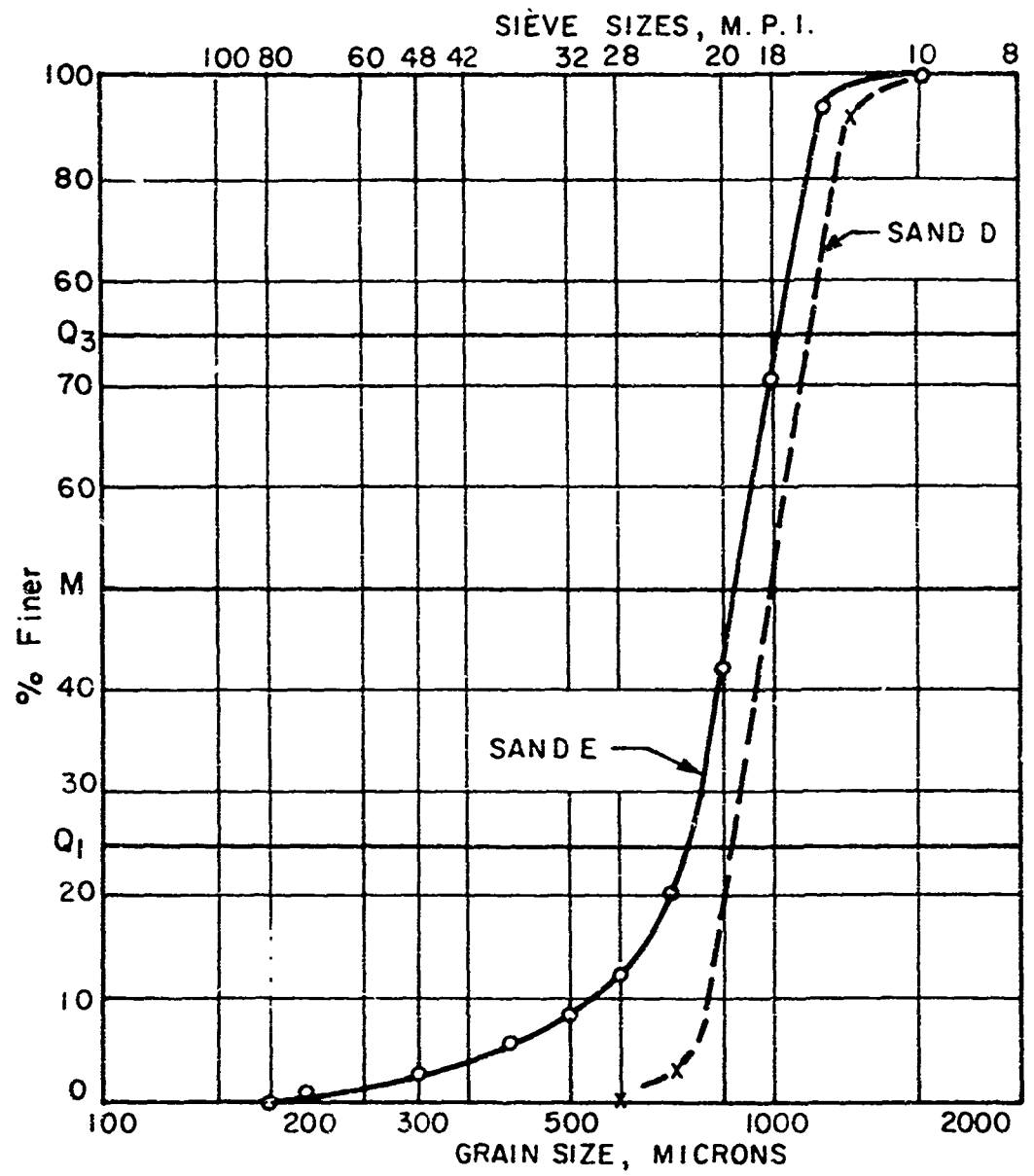


FIG. 13 MECHANICAL ANALYSIS OF SAND D & E  
(PRESENT STUDY)

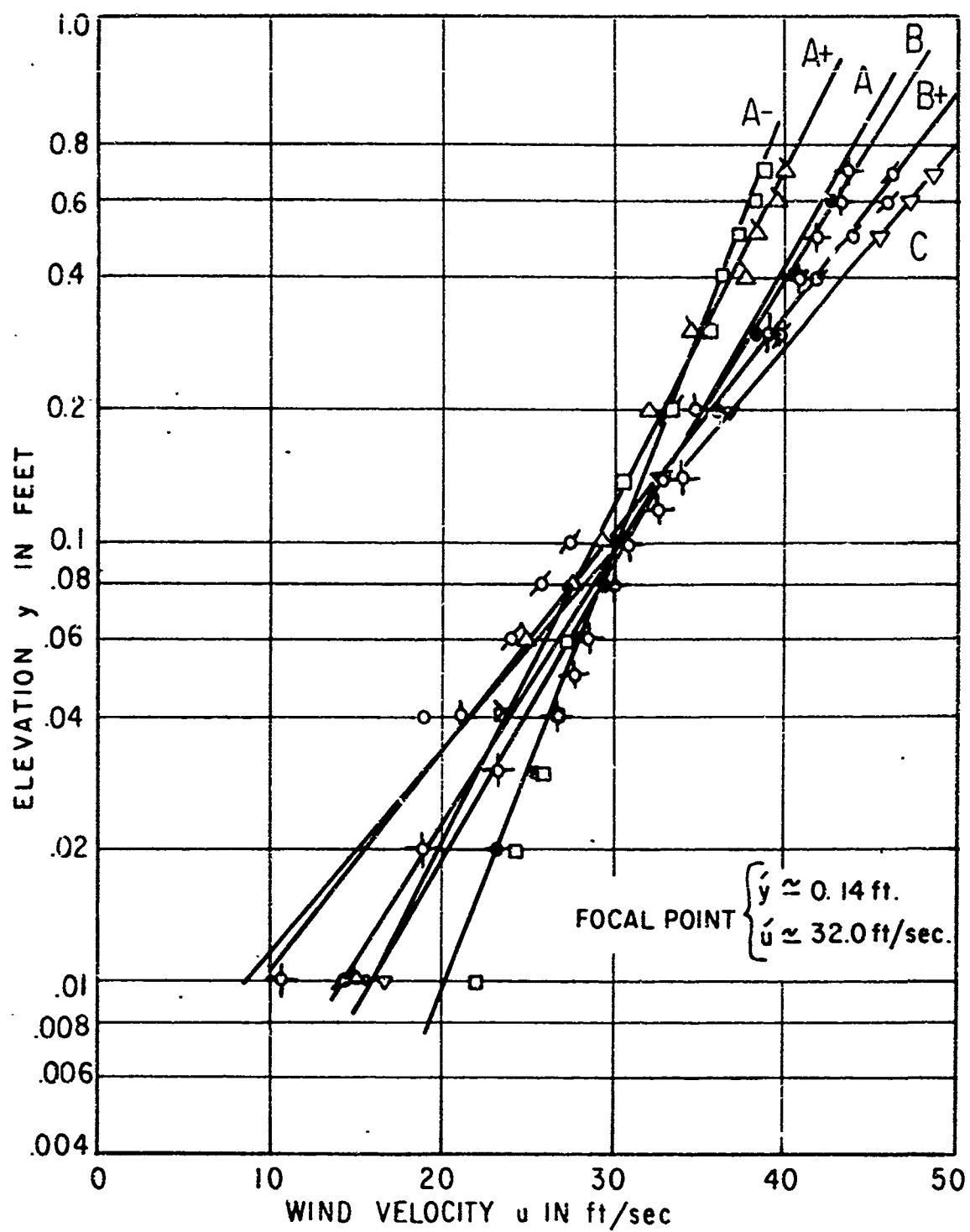


FIG. 14 VELOCITY DISTRIBUTION ABOVE SAND SURFACE WITH SAND MOVEMENT ( SAND D )



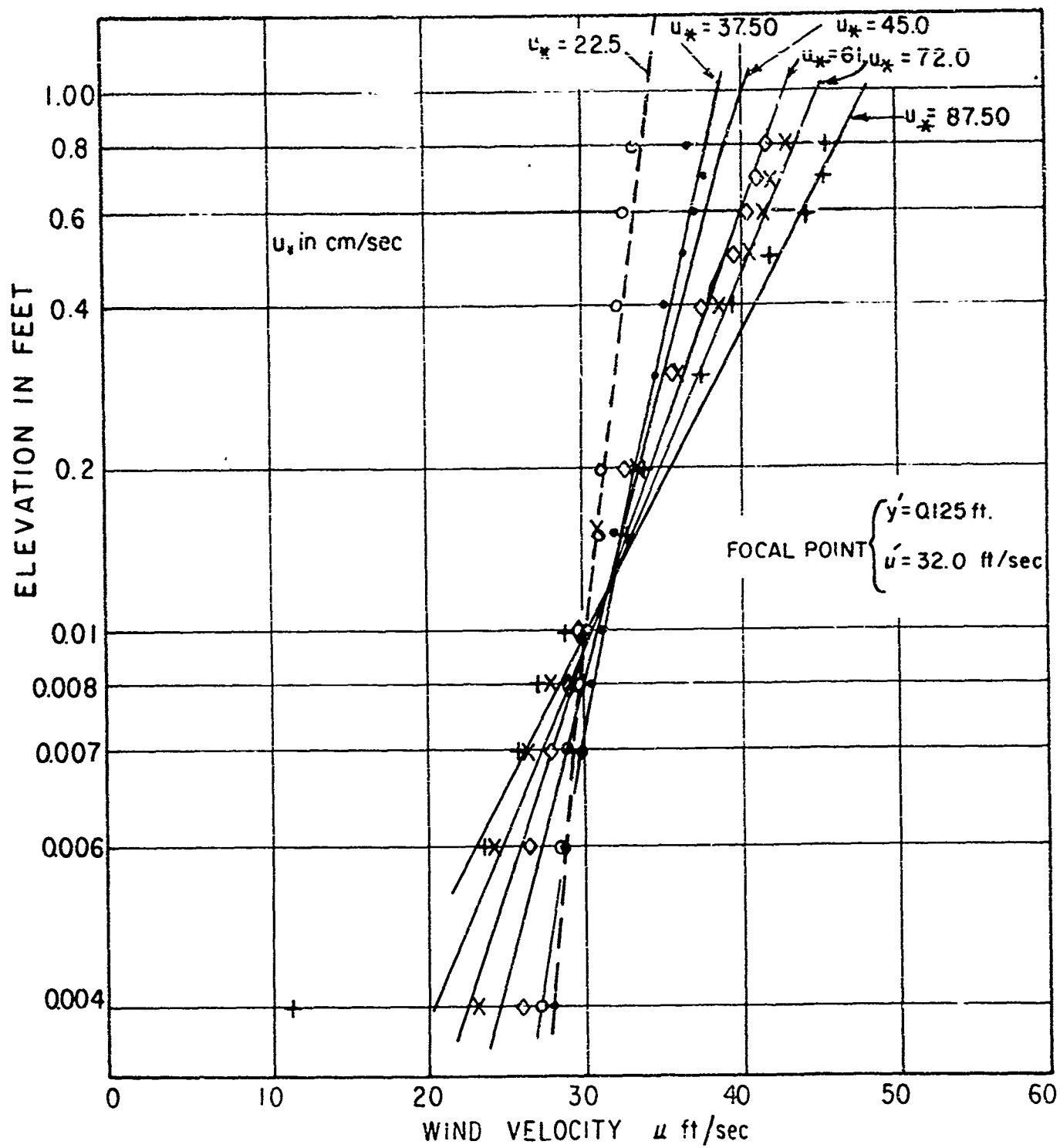


FIG. 15 VELOCITY DISTRIBUTION ABOVE SAND BED  
( WITH SAND MOVEMENT ) SAND E

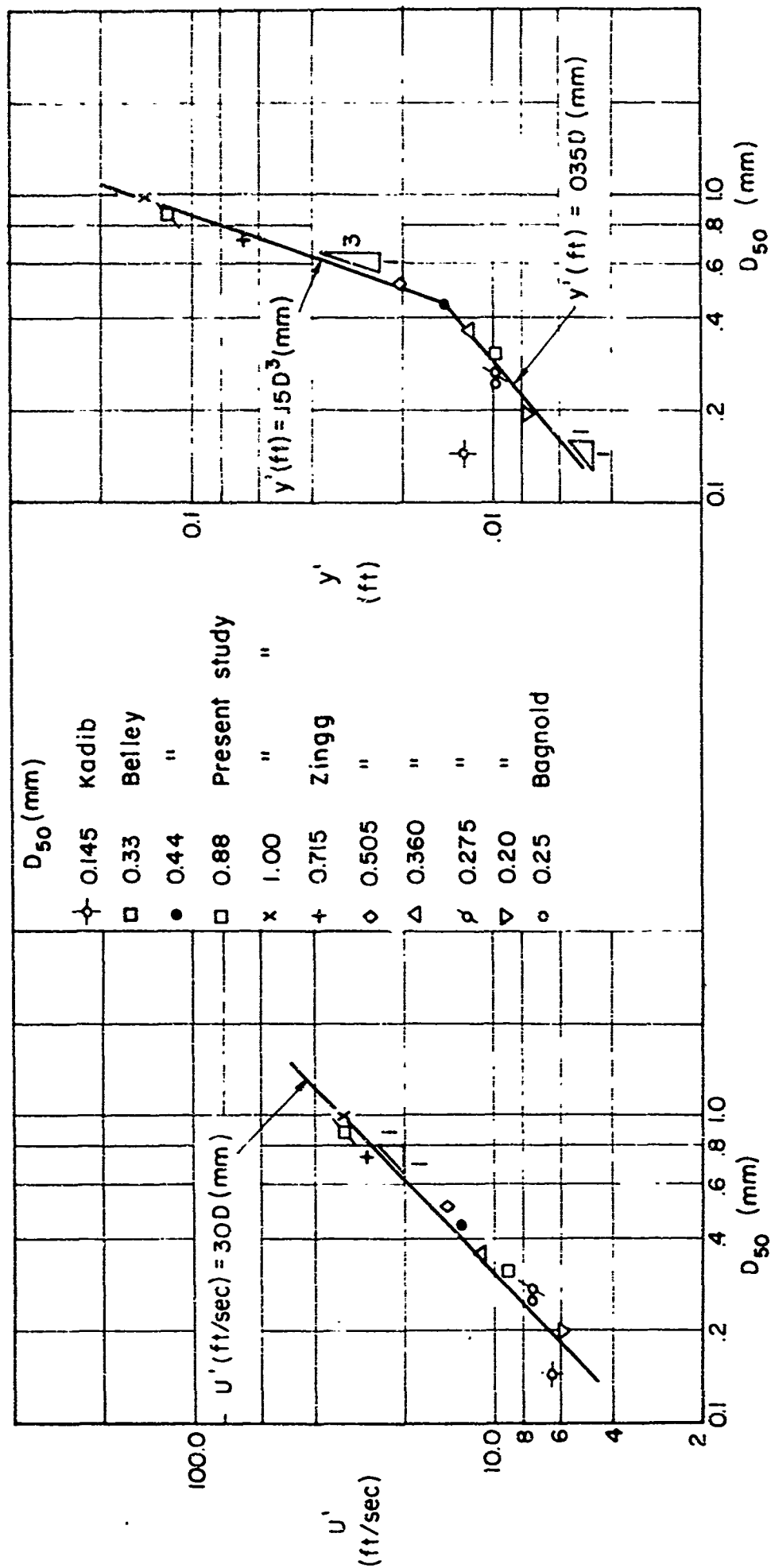


FIG. 16 RELATIONSHIP BETWEEN  $U'$  AND  $y'$  TO AVERAGE GRAIN DIAMETER  $D_{50}$

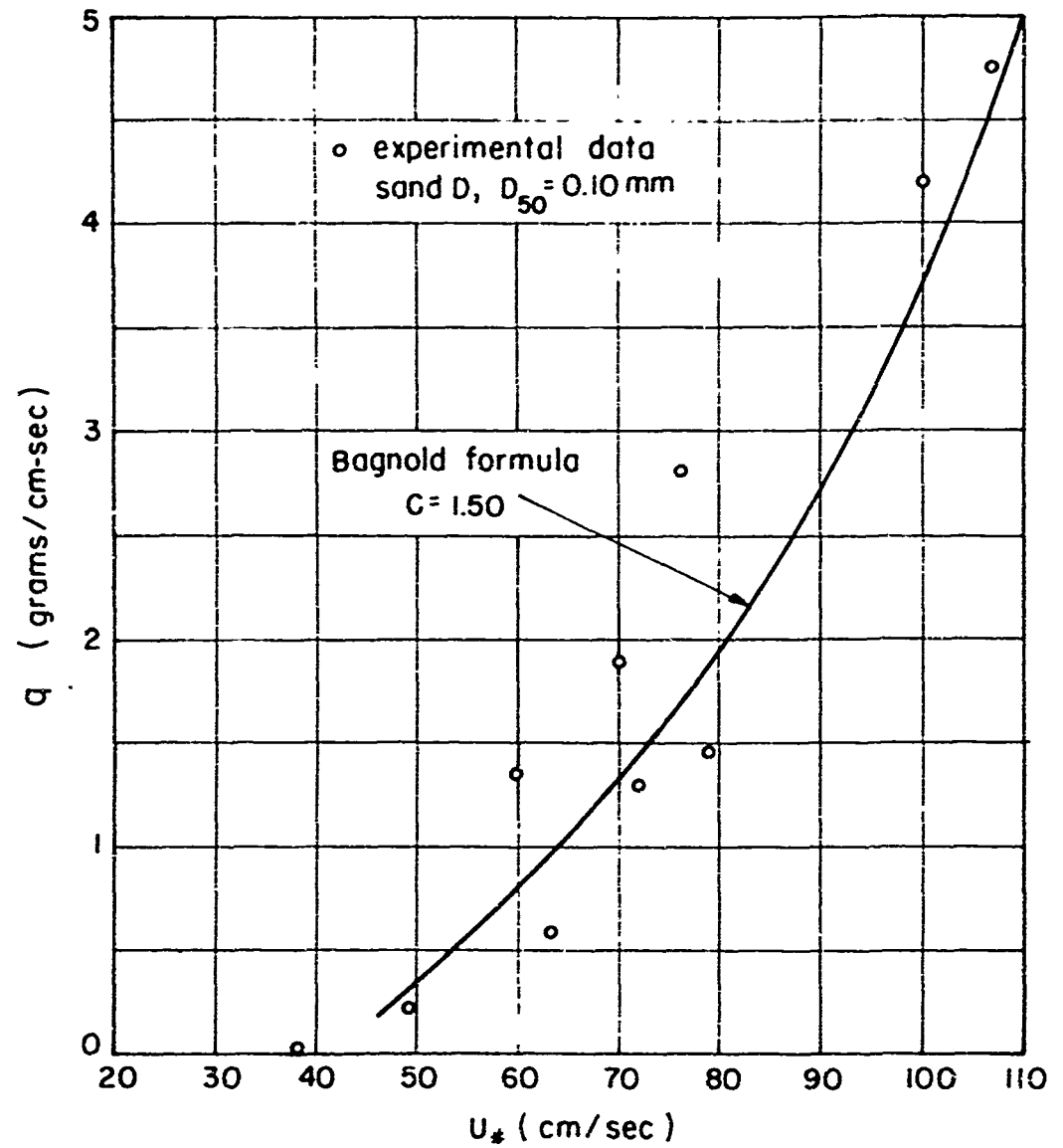


FIG.17 COMPARISON BETWEEN EXPERIMENTAL RESULTS AND BAGNOLD FORMULA (SAND D)

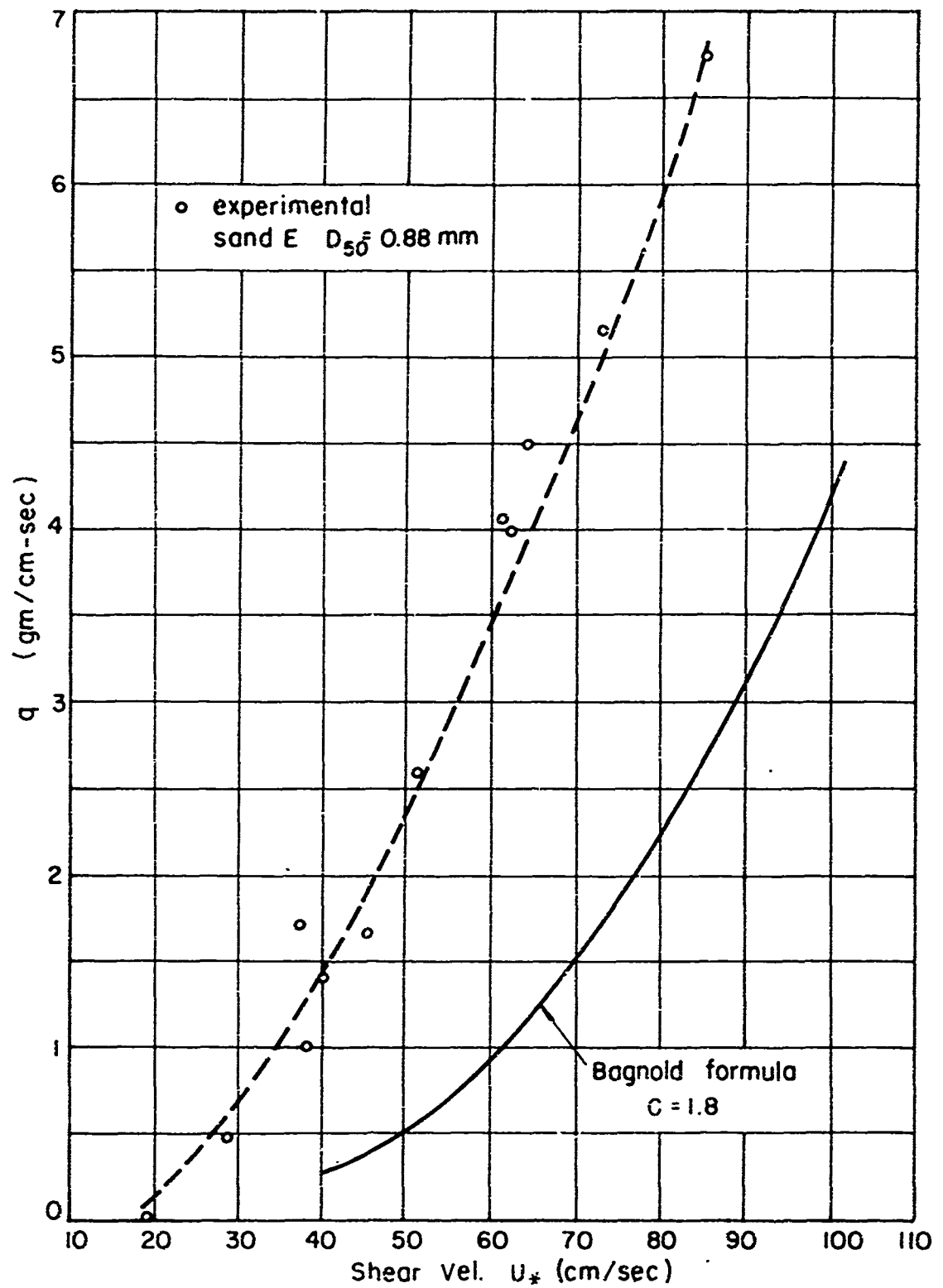


FIG. 18 COMPARISON BETWEEN EXPERIMENTAL RESULTS AND BAGNOLD FORMULA (SAND E)

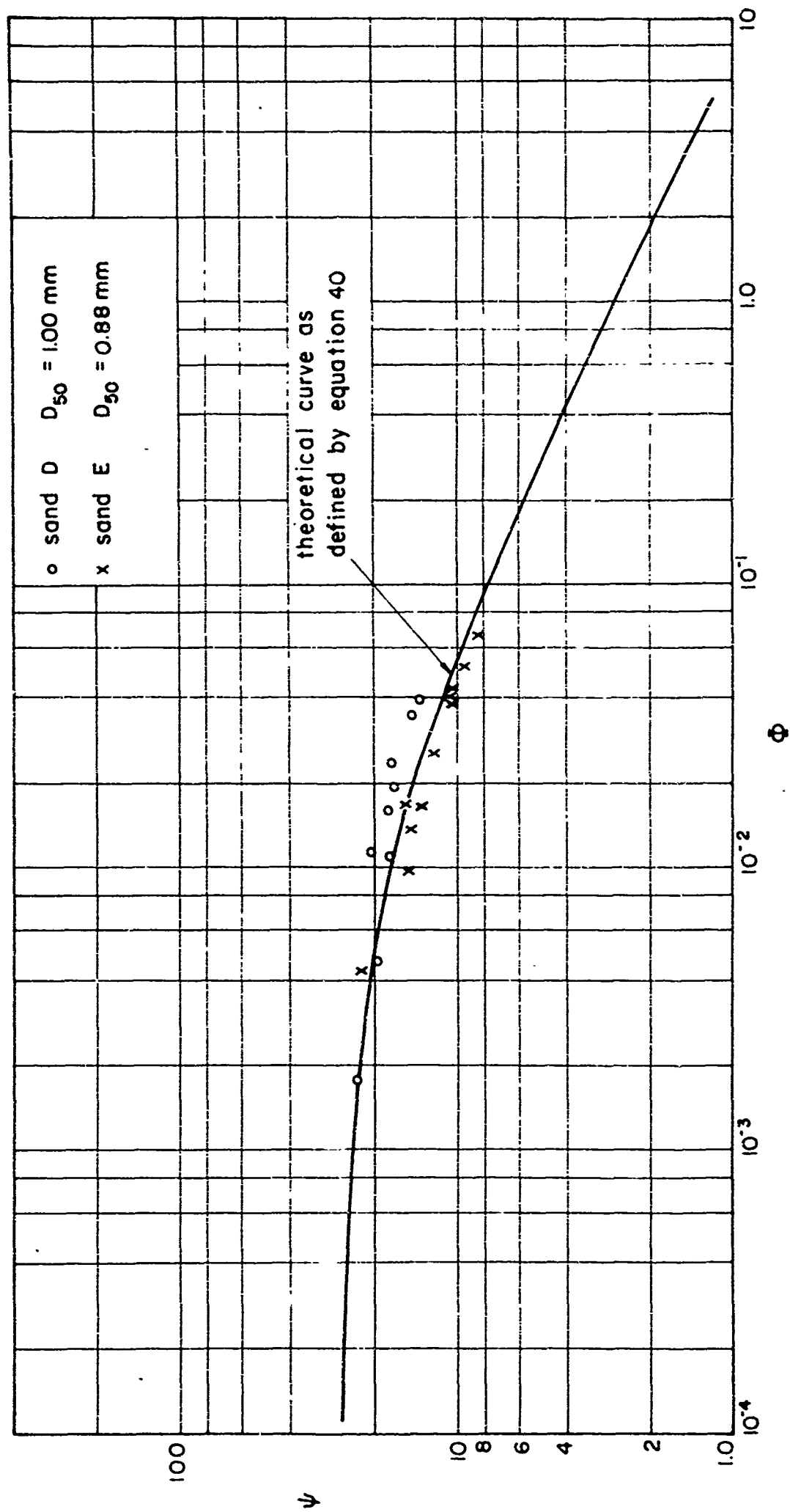
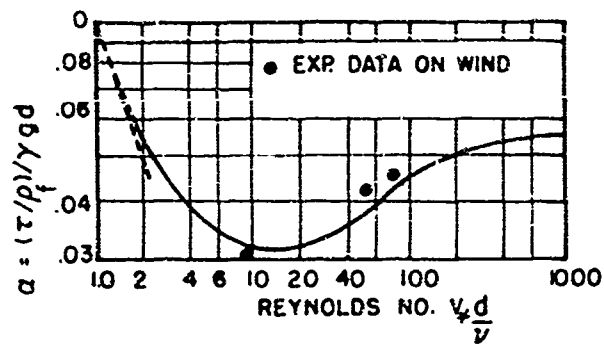


FIG.19 COMPARISON BETWEEN EXPERIMENTAL RESULTS AND PROPOSED METHOD (SAND D,E)



$$\gamma = \frac{\rho_s - \rho_f}{\rho_f}$$

$$d = D_{50}$$

FIG. 20 RELATION BETWEEN THRESHOLD SHEAR STRESS COEFFICIENT AND REYNOLDS NO. (AFTER SHIELDS)

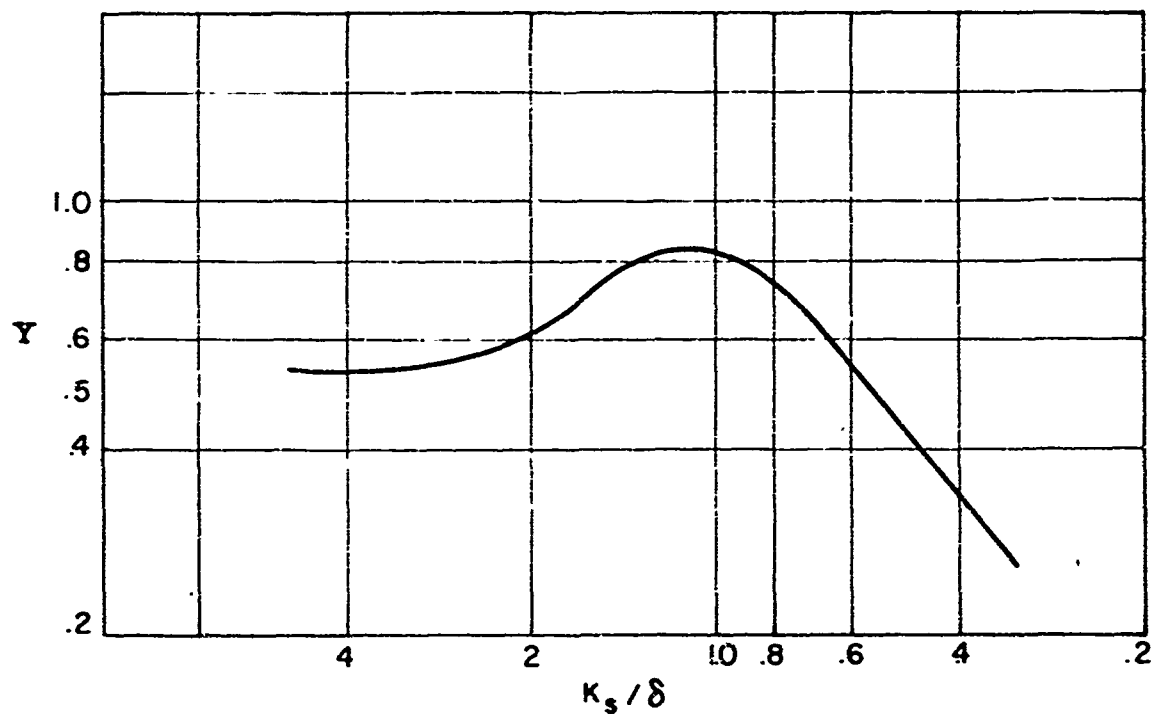


FIG. 21 CORRECTION  $Y$  FOR CHANGE IN THE LIFT COEFFICIENT DUE TO NON UNIFORM SEDIMENT (AFTER EINSTEIN)

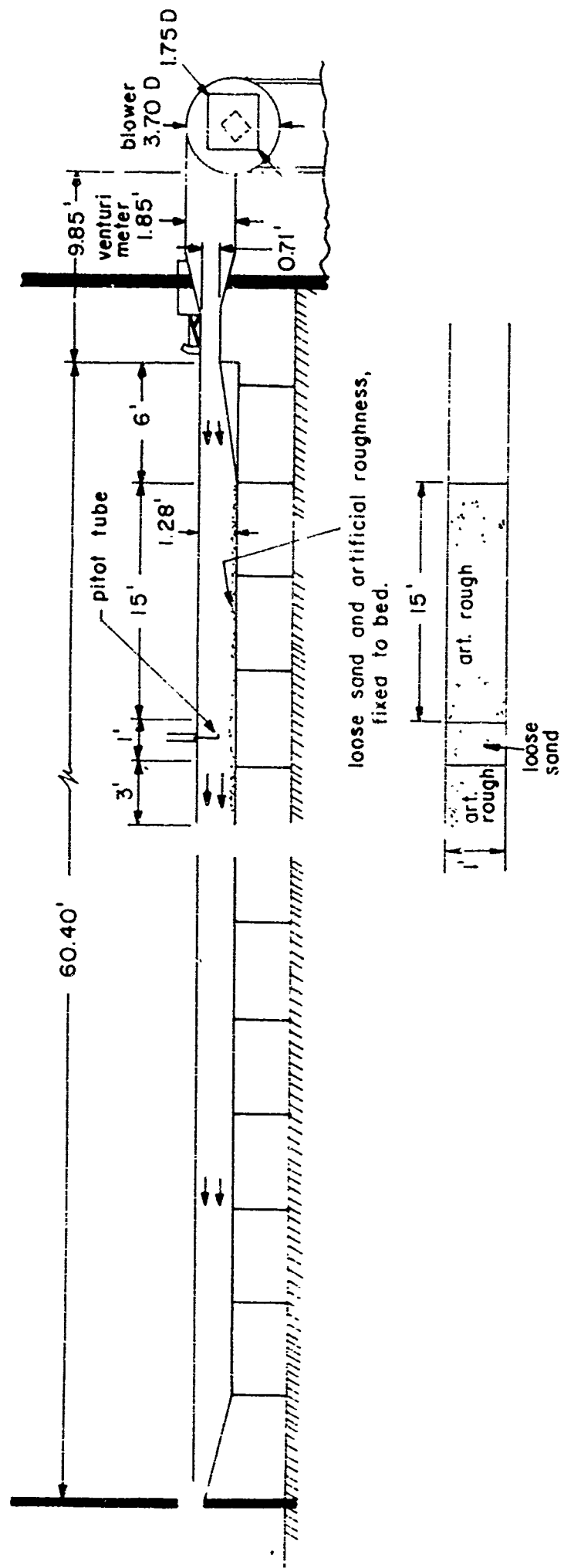


FIG. 22 WIND TUNNEL USED FOR SERIES b AND LAYOUT OF EXPERIMENT

## XV. TABLES



Table 1. Characteristics of the Available  
Experimental and Field Data on Sand  
Transport by Wind.

Sand	Tested by	date	Sorting C <sub>eff</sub> .S <sub>0</sub>	D <sub>50</sub> (mm)	wind tunnel dims.		
					Length (feet)	Width (feet)	Height (feet)
1	Bagnold	1936	1.00	0.250	30.0	1.00	2.50
2	Zingg	1942	-	0.200	56.00	area = 3 ft <sup>2</sup>	
3	Zingg	1942	-	0.275	56.00	area = 3 ft <sup>2</sup>	
4	Zingg	1942	-	0.360	56.00	area = 3 ft <sup>2</sup>	
5	Zingg	1942	-	0.505	56.00	area = 3 ft <sup>2</sup>	
6	Zingg	1942	-	0.715	56.00	area = 3 ft <sup>2</sup>	
7	Kawamura	1951	1.00	0.250	4.50	0.165	2.60
8	O'Brien & Rindlaub	1935	-	0.20	field measurements.		
9	Horikawa	1960	1.15	0.20	60	1.00	1.28
A	Belley	1962	1.23	0.44	100	4.0	2.50
B	Belley	1962	1.15	0.30	100	40	2.50
C	Kadib	1963	1.24	0.145	100	40	2.5

Table 2. Summary of the Available  
Experimental and Field Data on the  
Sand Transport rate  $q$  and the  
Shear Velocity  $U_*$ .

Sand number 1  
Bagnold, 1936  
 $D_{50} = 0.25$  mm

$U_*$	$q$
cm/sec	gm/cm-sec

19.2	0
25.0	0.029
40.40	0.118
50.50	0.25
62.00	0.44
88.00	1.22

Sand number 2  
Zingg 1941  
 $D_{50} = 0.20$  mm

$U_*$	$q$
cm/sec	gm/cm-sec

42.0	0.0382
46.3	0.0895
70.50	0.217
86.5	0.603
52.6	0.131
65.00	0.262
71.50	0.217
73.00	0.342
79.50	0.354
80.60	0.572
45.60	0.054

Sand number 3  
Zingg 1941  
 $D_{50} = 0.275$  mm

$U_*$	$q$
cm/sec	gm/cm-sec

60.00	0.187
70.00	0.304
86.50	0.505
89.50	0.83
42.50	0.075
58.00	0.167
63.60	0.30
74.50	0.605
85.00	0.78

Sand N.4  
Zingg 1941,  $D_{50} = 0.36$  mm

$U_*$	$q$
cm/sec	gm/cm-sec

50.2	0.187
62.00	0.329
63.50	0.42
73.00	0.67
81.00	0.905
77.00	0.738
74.50	0.575
68.00	0.475
60.00	0.385

Sand N.5  
Zingg 1941,  $D_{50} = 0.505$  mm

$U_*$	$q$
cm/sec	gm/cm-sec

58.0	0.284
67.0	0.545
80.0	0.746
83.0	1.03
101.0	1.67
62.0	0.48
76.5	0.610
60.5	0.319
91.0	1.29

Sand N.6  
Zingg, 1941  $D_{50} = 0.715$  mm

$U_*$	$q$
cm/sec	gm/cm-sec

81.00	1.27
102.0	2.28
77.50	0.975
97.00	1.92

Table 2 Continued

Sand N.7 Kawamura 1951 $D_{50} = 0.25$ mm		Sand 8* O'Brien and Rindlaub, $D_{50} = 0.20$ mm		Sand 9 Horikawa, 1960 $D_{50} = 0.20$ mm	
$U_*$ cm/sec	$q$ gm/cm-sec	$U_*$ cm/sec	$q$ gm/cm-sec	$U_*$ cm/sec	$q$ gm/cm-sec
27.0	0.01	37.00	0.378	26.8	0.0006
33.0	0.13	37.20	0.278	40.00	0.064
36.0	0.00	36.20	0.344	50.00	0.140
38.0	0.22	34.50	0.212	60.00	0.23
42.0	0.24	25.00	0.0875	70.00	0.33
46.0	0.40	23.80	0.074	80.00	0.52
54.0	0.65	21.50	0.0541	90.00	0.64
65.0	1.15	20.6	0.0464	100.00	0.83
73.0	1.60				
81.5	2.20				
87.0	2.75				
97.0	3.45				
109.0	4.30				

Sand A Belley 1962 $D_{50} = 0.44$ mm		Sand B, Belley 1962 $D_{50} = 0.30$ mm		Sand C, Kadib 1963 $D_{50} = 0.145$ mm	
$U_*$ cm/sec	$q$ gm/cm-sec	$U_*$ cm/sec	$q$ gm/cm-sec	$U_*$ cm/sec	$q$ gm/cm-sec
				22.0	0
				24.40	0.0017
				27.80	0.0277
				33.60	0.059
				36.80	0.088
30.0	0.012	16.00	0	41.0	0.144
35.0	0.105	33.00	0.25	59.5	0.189
38.0	0.182	38.00	0.32	62.6	0.270
39.0	0.220	41.00	0.36	64.50	0.365
41.0	0.232	44.00	0.39	73.00	0.475
46.0	0.380	49.00	0.50	76.00	0.53
50.0	0.506	59.0	0.74	79.00	0.649
55.00	0.780	66.0	0.93	80.50	0.736
64.00	1.180			84.00	0.95

\*These data are field measurements,  $U_*$  was calculated using equation 7 , since  $q$  was given as a function of wind speed 5 ft. above the bed.

Table 3. Summary of the Available Experimental data on the Coordinates of the Focal Point  $u'$  and  $z'$ .

Sand	Tested by	$D_{50}$ (mm)	$u'$ (ft/sec)	$y'$ (ft.)
2	Zingg	0.20	5.90	0.0075
3	Zingg	0.275	7.35	0.010
4	Zingg	0.36	11.00	0.012
5	Zingg	0.505	14.60	0.02
6	Zingg	0.715	26.00	0.070
A	Belley	0.440	13.00	0.0144
B	Belley	0.30	9.00	0.010
C	Kadib	0.145	6.40	0.0125

Table 4. Calculations for  $\frac{\psi \xi}{I} = \psi_*$  vs.  $\phi$   
relation as defined by equation (40).

Using equation 40 one can calculate  $\phi$  for chosen  $\frac{\psi \xi}{I}$  values and using the table of probability integrals using

$$A_* = 43.5$$

$$B_* = 0.143$$

$$\text{and } \frac{1}{\eta_0} = 2.00$$

$\psi_* = \frac{\psi \xi}{I}$	$\psi_* B_*$	$\psi_* B_* - \frac{1}{\eta_0}$	$\int_{\psi_* B_* - \frac{1}{\eta_0}}^{\infty} e^{-z^2} dz$	$\phi$
20.0	2.86	0.86	0.1952	0.0055
15.00	2.14	0.14	0.4442	0.0186
10.00	1.43	-0.57	0.716	0.058
5.00	0.715	-1.285	0.903	0.24
1.00	0.143	-1.857	0.968	6.95

Table 5. Necessary Calculations for the Corrections  $\xi$ ,  $I$  and  $\frac{\xi}{I}$

Sand 1 Bagnold,  $D_{50} = 0.25$  mm

cm/sec (1)	gm/cm - sec (2)	$\psi$ (3)	$\Phi$ (4)	$\psi_* = \frac{\psi \xi}{T}$ (5)	$\delta$ (mm) (6)	$\frac{D_{50}}{\delta}$ (7)	$\frac{D_{50}}{\chi}$ (8)	$\xi$ (9)	$I = \frac{\psi \xi}{\psi_*}$ (10)	$U_*^3 \frac{D^{3/2}}{\text{cm}^{4.5}/\text{sec}}$ (11)	$\frac{\xi}{I}$ (12)
25.0	0.029	85.1	$1.9 \times 10^{-3}$	21.40	0.681	0.366	0.264	20.0	79.40	61.70	0.252
40.40	0.118	32.4	$1.23 \times 10^{-2}$	15.90	0.422	0.59	0.426	7.60	15.50	262.0	0.490
50.50	0.25	20.9	$1.64 \times 10^{-2}$	14.90	0.337	0.74	0.533	4.80	6.70	509.0	0.712
62.00	0.44	13.80	$2.88 \times 10^{-2}$	12.90	0.275	0.785	0.564	3.20	3.42	943.0	0.935
88.00	1.22	6.87	$8.00 \times 10^{-2}$	8.80	0.194	1.28	0.926	1.53	1.19	2690.0	1.28

Table 5 (Con't)

Sand 2, Zingg  $D_{50} = 0.20$  mm

1	2	3	4	5	6	7	8	9	10	11	12
42.00	$3.82 \times 10^{-2}$	24.25	$3.93 \times 10^{-3}$	19.50	0.407	0.495	0.354	11.00	13.7	198.0	0.804
46.30	$8.95 \times 10^{-2}$	20.00	$9.2 \times 10^{-3}$	16.90	0.368	0.546	0.392	8.8	10.40	272.0	0.845
70.50	$2.17 \times 10^{-1}$	8.65	$2.23 \times 10^{-2}$	13.80	0.243	0.825	0.592	3.75	2.34	975.0	1.60
86.50	$6.03 \times 10^{-1}$	5.74	$6.2 \times 10^{-2}$	9.80	0.198	1.00	0.730	2.50	1.46	1840.0	1.71
52.60	$1.31 \times 10^{-1}$	15.50	$1.35 \times 10^{-2}$	15.50	0.326	0.616	0.443	7.00	6.95	396.0	1.00
65.00	$2.62 \times 10^{-1}$	10.10	$2.7 \times 10^{-2}$	13.00	0.264	0.76	0.546	4.50	3.50	765.0	1.29
71.50	$2.17 \times 10^{-1}$	8.40	$2.23 \times 10^{-2}$	13.80	0.240	0.835	0.600	3.80	2.30	1030.0	1.64
73.00	$3.42 \times 10^{-1}$	8.05	$3.52 \times 10^{-2}$	12.00	0.234	0.855	0.615	3.60	2.42	1090.0	1.49
79.5	$3.54 \times 10^{-1}$	6.76	$3.64 \times 10^{-2}$	11.90	0.215	0.93	0.670	3.00	1.71	1400.0	1.76
80.6	$5.72 \times 10^{-1}$	6.60	$5.9 \times 10^{-2}$	9.90	0.212	0.945	0.680	2.80	1.87	1490.0	1.50
45.6	$5.85 \times 10^{-1}$	20.60	$6.2 \times 10^{-3}$	18.00	0.375	0.536	0.386	9.00	10.25	266.0	0.873

Table 5 (Con't)

Sand 3 Zingg  $D_{50} = 0.275$  mm

1	2	3	4	5	6	7	8	9	10	11	12
60	0.187	16.4	$1.05 \times 10^{-2}$	16.00	0.286	0.965	0.695	2.70	2.78	975.0	0.975
70	0.304	12.00	$1.7 \times 10^{-2}$	14.80	0.244	1.13	0.812	2.00	1.62	1560.0	1.23
86.5	0.505	7.90	$2.83 \times 10^{-2}$	13.00	0.197	1.39	1.000	1.30	0.795	2920.0	1.65
89.5	0.830	7.36	$4.65 \times 10^{-2}$	10.70	0.191	1.45	1.040	1.20	0.825	3280.0	1.45
42.50	0.075	32.70	$4.17 \times 10^{-3}$	18.50	0.40	0.487	0.495	5.50	9.75	346.0	0.565
58.00	0.167	17.50	$9.35 \times 10^{-3}$	16.80	0.295	0.93	0.670	3.00	3.12	885.0	0.955
63.60	0.300	14.60	$1.62 \times 10^{-2}$	14.80	0.269	1.02	0.736	2.50	2.47	1160.0	1.01
74.50	0.605	10.60	$3.39 \times 10^{-2}$	12.30	0.230	1.19	0.86	1.75	1.51	1910.0	1.16
85.00	0.78	8.20	$4.6 \times 10^{-2}$	11.00	0.201	1.37	0.985	1.35	1.01	2780.0	1.34

Sand 4 Zingg and  $D_{50} = 0.36$  mm

50.2	0.187	30.30	$7.09 \times 10^{-3}$	17.50	0.339	1.06	0.764	2.23	3.86	867.0	0.577
62.0	0.329	20.00	$1.47 \times 10^{-2}$	15.20	0.276	1.30	0.94	1.50	1.98	1590	0.760
63.50	0.42	19.30	$1.58 \times 10^{-2}$	15.00	0.269	1.34	0.962	1.40	1.30	1740	0.777
73.00	0.67	14.50	$2.52 \times 10^{-2}$	13.20	0.234	1.53	1.10	1.10	1.21	2620.0	0.910
81.00	0.905	11.70	$3.3 \times 10^{-2}$	12.20	0.211	1.71	1.23	0.84	0.795	3540.0	1.041
77.00	0.738	13.00	$2.77 \times 10^{-2}$	13.00	0.222	1.63	1.17	0.95	0.95	3060.0	1.000
74.50	0.575	13.90	$2.16 \times 10^{-2}$	14.00	0.23	1.57	1.13	1.00	0.995	2800.0	1.007
68.00	0.475	16.80	$1.785 \times 10^{-2}$	14.50	0.251	1.43	1.03	1.22	1.41	2150.0	0.863
60.00	0.385	21.40	$1.45 \times 10^{-2}$	22.50	0.285	1.26	0.91	1.60	1.55	1470.0	1.030

Sand 5 Zingg  $D_{50} = 0.505$ 

58.00	0.284	32.20	$6.42 \times 10^{-3}$	18.00	0.295	1.71	1.23	0.950	1.70	2170.0	0.558
67.00	0.545	24.20	$1.27 \times 10^{-2}$	15.900	0.256	1.97	1.42	0.65	0.995	3340.0	0.652
80.00	0.746	16.90	$1.69 \times 10^{-2}$	14.90	0.214	2.36	1.695	0.44	0.50	5780.0	0.981
83.00	1.03	15.65	$2.33 \times 10^{-2}$	13.50	0.706	2.46	1.760	0.41	0.473	6450.0	0.861
101.00	1.67	10.60	$3.78 \times 10^{-2}$	11.80	0.169	3.00	2.15	0.28	0.25	1135.0	1.112
62.00	0.48	28.20	$1.09 \times 10^{-2}$	16.10	0.276	1.82	1.310	0.74	1.29	2660.0	0.571
76.50	0.610	18.50	$1.385 \times 10^{-2}$	15.10	0.224	2.26	1.62	0.48	0.59	4970.0	0.815
60.50	0.319	29.60	$7.22 \times 10^{-3}$	17.50	0.283	1.78	1.28	0.80	1.35	2450.0	0.591
91.00	1.29	13.02	$2.92 \times 10^{-2}$	13.00	0.188	2.68	1.93	0.34	0.342	8000.0	0.998



Table 5 (Con't)

Sand 6 Zingg,  $D_{50} = 0.715$  mm

1	2	3	4	5	6	7	8	9	10	11	12
81.00	1.27	23.40	$1.72 \times 10^{-2}$	14.5	0.212	3.36	2.42	0.23	0.37	$1.04 \times 10^4$	0.620
102.0	2.28	14.70	$3.1 \times 10^{-2}$	12.5	0.168	4.25	3.05	0.14	0.165	$2.04 \times 10^4$	0.850
77.50	0.975	25.20	$1.32 \times 10^{-2}$	15.50	0.220	3.25	2.34	0.21	0.34	$8.9 \times 10^4$	0.615
97.50	1.920	16.20	$2.6 \times 10^{-2}$	13.00	0.176	4.05	2.92	0.15	0.187	$1.74 \times 10^4$	0.806

Sand 8, O'Brien and Rindlaub,  $D_{50} = 0.20$  mm (field measurements)

53.50	0.378	14.90	$3.46 \times 10^{-2}$	12.1	0.318	0.63	0.452	6.8	8.38	433.0	0.812
53.90	0.278	14.60	$2.54 \times 10^{-2}$	13.2	0.316	0.635	0.455	6.7	7.40	444.0	0.904
52.20	0.344	15.60	$3.15 \times 10^{-2}$	12.4	0.326	0.615	0.441	7.00	8.80	404.	0.795
49.00	0.212	17.80	$1.94 \times 10^{-2}$	14.2	0.348	0.575	0.413	8.2	10.3	333.0	0.797
32.90	0.0875	39.20	$8.00 \times 10^{-3}$	17.20	0.518	0.387	0.278	18.0	41.0	101.0	0.439
30.80	0.0740	44.80	$6.77 \times 10^{-3}$	17.8	0.553	0.352	0.260	21.0	52.8	82.8	0.397
26.90	0.0541	58.80	$4.95 \times 10^{-3}$	18.7	0.634	0.317	0.227	27.5	86.6	55.1	0.318
25.40	0.0464	65.5	$4.25 \times 10^{-3}$	19.3	0.670	0.300	0.215	34.0	115.5	46.7	0.294

Sand A, Belley,  $D_{50} = 0.44$  mm

35.0	0.105	75.00	$2.92 \times 10^{-3}$	20.00	0.49	0.900	0.65	1.90	7.10	390.0	0.267
38.0	0.182	64.00	$5.05 \times 10^{-3}$	19.00	0.45	0.98	0.705	1.65	5.54	532.0	0.297
39.0	0.220	60.50	$6.10 \times 10^{-3}$	18.00	0.44	1.00	0.72	1.60	5.36	545.0	0.298
41.0	0.232	55.00	$6.45 \times 10^{-3}$	18.00	0.42	1.05	0.76	1.50	4.56	625.0	0.327
46.0	0.380	43.80	$1.06 \times 10^{-2}$	16.50	0.372	1.18	0.82	1.30	3.46	885.0	0.376
50.0	0.506	36.80	$1.41 \times 10^{-2}$	15.50	0.342	1.28	0.92	1.20	2.85	1150.0	0.421
55.00	0.780	30.60	$2.17 \times 10^{-2}$	14.20	0.312	1.42	1.02	1.15	2.50	1520.0	0.464
64.00	1.180	21.50	$3.28 \times 10^{-2}$	17.20	0.768	1.64	1.18	1.08	1.85	2400.0	0.659

Table 5 (Con't)

Sand B, Belley,  $D_{50} = 0.30$  mm

1	2	3	4	5	6	7	8	9	10	11	12
33.0	0.25	59.0	1.23x10 <sup>-2</sup>	16.50	0.52	0.58	0.42	6.00	21.40	187.0	0.28
38.00	0.32	44.50	1.58x10 <sup>-2</sup>	15.50	0.45	0.67	0.48	3.70	10.60	280.0	0.348
41.0	0.36	38.20	1.78x10 <sup>-2</sup>	15.0	0.416	0.72	0.52	3.50	8.90	354.0	0.392
44.0	0.39	33.00	1.92x10 <sup>-2</sup>	14.50	0.390	0.77	0.55	3.00	6.80	435.0	0.439
49.0	0.50	26.80	2.46x10 <sup>-2</sup>	13.80	0.350	0.81	0.59	2.40	4.65	605.0	0.515
59.0	0.74	18.40	3.66x10 <sup>-2</sup>	13.00	0.290	1.03	0.74	1.50	2.12	1060.0	0.706
66.00	0.93	14.70	4.6x10 <sup>-2</sup>	11.00	0.26	1.15	0.83	1.30	1.73	1470.0	0.748
Sand C, Kadib, $D_{50} = 0.145$ mm											
24.4	0.0017	51.80	2.52x10 <sup>-4</sup>	25.00	0.698	0.208	0.149	66.00	137.0	25.40	0.483
27.80	0.0277	40.0	4.11x10 <sup>-3</sup>	19.50	0.613	0.237	0.170	50.00	102.5	37.5	0.487
33.60	0.059	27.4	8.75x10 <sup>-2</sup>	17.00	0.506	0.287	0.206	34.00	55.3	66.2	0.62
36.80	0.088	22.70	1.31x10 <sup>-2</sup>	15.60	0.463	0.315	0.225	28.00	40.6	87.30	0.787
41.00	0.144	18.30	2.14x10 <sup>-2</sup>	13.90	0.416	0.348	0.250	22.50	29.6	120.5	0.760
59.5	0.189	8.70	2.81x10 <sup>-2</sup>	13.0	0.286	0.506	0.364	10.20	6.81	368.0	1.49
62.6	0.270	7.84	4.01x10 <sup>-2</sup>	11.50	0.272	0.535	0.383	9.40	6.40	430.0	1.39
64.5	0.365	7.42	5.42x10 <sup>-2</sup>	10.10	0.264	0.550	0.395	8.80	6.47	468.0	1.36
73.00	0.475	5.80	7.05x10 <sup>-2</sup>	9.20	0.234	0.62	0.445	6.90	4.35	680.0	1.30
76.00	0.530	5.32	7.86x10 <sup>-2</sup>	8.80	0.224	0.65	0.465	6.40	3.87	770.0	1.65
79.00	0.645	4.95	9.57x10 <sup>-2</sup>	8.10	0.216	0.67	0.482	5.90	3.60	862.0	1.64
80.50	0.736	4.75	1.09x10 <sup>-1</sup>	7.70	0.212	0.584	0.491	5.70	3.52	913.0	1.62
84.00	0.950	4.37	1.41x10 <sup>-1</sup>	6.8	0.203	0.715	0.513	5.20	3.34	1038.0	1.55
Sand 9, Horikawa, $D_{50} = 0.20$ mm											
26.8	0.0006	56.2	5.49x10 <sup>-5</sup>	25.00	0.636	0.314	0.226	28.0	62.70	56.10	0.445
40.0	0.0640	26.0	5.85x10 <sup>-3</sup>	18.20	0.426	0.47	0.338	10.2	14.60	181.0	0.700
50.0	0.140	16.60	1.28x10 <sup>-2</sup>	15.80	0.341	0.586	0.422	7.80	8.20	354.0	0.592
60.0	0.230	11.50	2.1x10 <sup>-2</sup>	14.00	0.284	0.705	0.506	5.30	4.36	611.0	1.22
70.0	0.330	8.48	3.02x10 <sup>-2</sup>	12.60	0.244	0.820	0.590	3.80	2.56	970.0	1.49
80.0	0.520	6.50	4.76x10 <sup>-2</sup>	10.80	0.213	0.940	0.675	2.95	1.78	1450.0	1.66
90.0	0.640	5.13	5.85x10 <sup>-2</sup>	10.00	0.189	1.06	0.761	2.30	1.18	2060.0	1.95
100.0	0.830	4.16	7.60x10 <sup>-2</sup>	9.00	0.170	1.18	0.846	1.85	0.78	2828.0	2.16

Table 6. Experimental Results on Sand D and E  
(present study)

Sand D ( $D_{50} = 1.00$ mm)		Sand E ( $D_{50} = 0.88$ mm)	
$U_*$ cm sec	$q$ gm cm-sec	$U_*$ cm/sec	$q$ gm/cm-sec
		28.5	0.46
48.75	0.215	37.00	1.71
71.60	1.31	37.50	1.00
60.00	1.36	40.0	1.40
78.60	2.37	45.0	1.65
100.00	4.20	51.00	2.60
107.0	4.75	61.00	4.10
63.6	0.59	62.00	4.00
70.0	1.925	64.00	4.50
76.20	2.87	72.00	5.15
		85.0	6.74

Table 7. Determination of  $\psi_*$  and  $\phi$  from  
Experimental Data  
(Sand D)

Sand D

$$D_{50} = 1.00 \text{ mm}$$

$$\frac{\rho_s - \rho_f}{\rho_f} gD = 2.14 \times 10^5, \quad \psi = \frac{2.14 \times 10^5}{U_*^2}$$

$$D^{3/2} = \left(\frac{1}{10}\right)^{3/2} = 0.0316 \text{ cm}^{3/2}$$

$$\phi = \frac{q}{D^{3/2}} = 2.59 \times 10^{-4}$$

$$= 8.20 \times 10^{-3} q$$

$U_*$ cm/sec	$q$ gm/cm-sec	$\psi$	$\frac{\xi}{I}^*$	$\psi \frac{\xi}{I} = \psi_*$	$\phi$
48.75	0.215	90.10	0.25	22.50	$1.76 \times 10^{-3}$
71.60	1.310	41.80	0.42	17.50	$1.07 \times 10^{-2}$
60.00	1.360	59.40	0.34	20.5	$1.12 \times 10^{-2}$
78.60	2.370	34.60	0.49	16.90	$1.95 \times 10^{-2}$
100.00	4.200	21.40	0.68	14.50	$3.45 \times 10^{-2}$
107.00	4.750	18.20	0.75	13.60	$3.9 \times 10^{-2}$
63.60	0.590	52.9	0.365	19.3	$4.84 \times 10^{-3}$
70.00	1.925	43.6	0.410	17.9	$1.60 \times 10^{-2}$
76.20	2.87	36.9	0.47	17.3	$2.36 \times 10^{-2}$

\* The values of  $\frac{\xi}{I}$  were obtained from Figure 9.

Table 8. Determination of  $\psi_*$  and  $\phi$  to be  
Compared with the Theoretical Values  
(Sand E)

$$D_{50} = 0.88 \text{ mm}$$

$$\frac{\rho_s - \rho_f}{\rho_f} = gD = 1.88 \times 10^5$$

$$D^{3/2} = \left(\frac{8.8}{100}\right)^{3/2} = 2.6 \times 10^{-2} \text{ cm}^{3/2}$$

$$\begin{aligned} \phi &= \frac{q}{D^{3/2}} = 2.56 \times 10^{-4} \\ &= 0.986 \times 10^{-2} q \end{aligned}$$

$U_*$ cm/sec	$q$ qm/cm sec	$\psi$	$\xi/I^*$	$\delta$ (mm)	$\frac{D_{50}}{\delta}$	** Y	$\frac{\xi Y}{I}$	$\psi$	$\phi$
28.5	0.46	230.0	0.132	0.600	1.47	0.74	22.00	$4.52 \times 10^{-3}$	
37.00	1.71	137.0	0.180	0.462	1.91	0.62	15.20	$1.685 \times 10^{-2}$	
37.50	1.00	134.0	0.190	0.455	1.94	0.62	15.80	$9.86 \times 10^{-3}$	
40.00	1.40	117.50	0.210	0.428	2.06	0.60	14.90	$1.38 \times 10^{-2}$	
45.00	1.65	92.50	0.255	0.380	2.32	0.57	13.50	$1.625 \times 10^{-2}$	
51.00	2.60	72.50	0.300	0.336	2.63	0.55	12.10	$2.56 \times 10^{-2}$	
61.00	4.10	50.6	0.380	0.280	3.15	0.54	10.60	$4.08 \times 10^{-2}$	
62.00	4.00	49.00	0.390	0.276	3.18	0.54	10.30	$3.98 \times 10^{-2}$	
64.00	4.50	46.00	0.410	0.267	3.30	0.54	10.20	$4.49 \times 10^{-2}$	
72.00	5.15	36.3	0.48	0.238	3.70	0.53	9.25	$5.14 \times 10^{-2}$	
85.00	6.75	26.0	0.60	0.201	4.38	0.53	8.30	$6.65 \times 10^{-2}$	

\* The values of  $\frac{\xi}{I}$  were obtained from Figure 9

\*\* The Y values were obtained from Figure 21

Table 9. Calculations for Sand Transport (in land)  
using the Proposed Method for Reach 8, Salmon Beach, California

$U_{18}$ ft. ft/sec (1)	$U_*$ cm/sec (2)	$\psi$ (3)	$\frac{U_*}{U_{18}}$ (4)	$\psi_*$ (5)	$\phi$ (6)	$q$ gm/cm-sec (7)
18.2	0.40*			>25	0	0
18.8	1.60*			>25	0	0
20.00	4.00*	No calculation are necessary, since there is no motion.		>25	0	0
21.00	6.00*			>25	0	0
21.80	7.60*			>25	0	0
22.90	9.80*			>25	0	0
23.20	10.40*			>25	0	0
24.70	13.40*			>25	0	0
26.20	16.40*			>25	0	0
26.60	17.20*			>25	0	0
27.60	19.20*			>25	0	0
28.40	20.80*			>25	0	0
29.10	22.20	250.0	0.125	31.20	0	0
30.30	24.60	205.0	0.145	29.80	0	0
32.00	28.00	158.0	0.170	26.80	0	0
33.20	30.40	139.0	0.195	27.00	0	0
34.70	33.40	111.0	0.220	24.40	$4.5 \times 10^{-4}$	0.0246
36.00	36.60	92.80	0.250	23.20	$1.1 \times 10^{-3}$	0.06
37.80	39.6	79.50	0.275	21.80	$2.21 \times 10^{-3}$	0.12
39.30	42.60	63.00	0.325	20.60	$3.5 \times 10^{-3}$	0.190
40.70	45.40	60.00	0.340	20.4	$3.7 \times 10^{-3}$	0.200
>41.2	46.40	58.60	0.345	20.00	$4 \times 10^{-3}$	0.218

\*Those values were used to compare with calculations using Bagnold formula as shown in reference (7).

Table 9 (Con't)

North $\ell_r = 900'$		Northwest $\ell_r = 1700'$		West $\ell_r = 1400'$		Southwest $\ell_r = 1400'$		Q total inland	
t hrs (8)	Q (9)	t hrs (8)	Q (9)	t hrs (8)	Q (9)	t hrs (8)	Q (9)	in lb year	

No calculations are  
necessary, since there  
is no motion.

8	$4.4 \times 10^{-4}$	10	$9.55 \times 10^4$	1	$0.86 \times 10^4$	1	$0.31 \times 10^4$	$15.12 \times 10^4$
2	$2.7 \times 10^4$	14	$35.5 \times 10^4$	0	0	3	$2.24 \times 10^4$	$40.44 \times 10^4$
8	$2.03 \times 10^5$	3	$1.52 \times 10^5$	0	0	0	0	$35.50 \times 10^4$
8	$3.4 \times 10^5$	5	$4.00 \times 10^5$	0	0	3	$7.1 \times 10^4$	$81.10 \times 10^4$
3	$1.35 \times 10^5$	2	$1.69 \times 10^4$	0	0	0	0	$30.40 \times 10^4$
5	$2.44 \times 10^5$	1	$9.2 \times 10^4$	0	0	0	0	$33.6 \times 10^4$

$Q_t$  Total =

$\Sigma 2.3616 \times 10^6$   
#/yr